UNIVERSITY OF CALIFORNIA

SANTA CRUZ

MELANOCORTINS OF THE CENTRAL NERVOUS SYSTEM: STRUCTURAL INSIGHTS ON PIGMENTATION AND APPETITE.

A dissertation submitted in partial satisfaction of
The requirements for the degree of

DOCTOR OF PHILOSOPHY

in

CHEMISTRY

by

Michael E. Madonna

March 2012

The Dissertation of Michael E. Madonna
is approved:

_____
Professor Glenn L. Millhauser, Advisor

_____
Professor Theodore R. Holman, Chair

_____
Professor Seth M. Rubin

_____
Tyrus Miller
Vice Provost and Dean of Graduate Studies

Table of Contents

List of Figures:

General Introduction:

Chapter 2:

List of Tables:

Chapter 3:

Chapter 5:

Melanocortins of the Central Nervous System: Structural Insights on Pigmentation and Appetite

Michael E. Madonna

Abstract

The Melanocortin system of G-Protein coupled receptors and ligands plays a vital role in cell signaling of many important physiological processes, including pigmentation, steroidogenesis, and metabolic control. These receptors are all activated by ligands derived from the proopiomelanocortin (POMC). This prohormone is processed by tissue specific expression of various proteases. Three receptors within this system have a secondary level of regulation. Melanocortin receptors (McRs) 1, 3 and 4 also respond to endogenously expressed antagonist proteins, the agouti-signaling protein (ASIP) and agouti-related protein (AgRP). ASIP and AgRP compete with POMC ligands for receptor binding and signal for reduction in cAMP. Both antagonists are sequentially and structurally similar; yet show differing tissue expression and receptor binding specificities. AgRP is expressed in the hypothalamus and signals for an increase in appetite and lower energy expenditure through Mc3R and Mc4R. ASIP is primarily expressed in the skin and affects pigmentation through Mc1R, but can interact with Mc3R and Mc4R through some genetic mutations.

The ligand expression and binding specificity at McRs 1, 3 and 4 provide a unique set of tools for understanding structural determinants required for regulation of pigmentation and energy balance and homeostasis. Here study a novel third

antagonist sequence, AgRP2, discovered in teleost fish and expressed in the light sensitive Pineal gland of the brain. This protein shares the same cysteine spacing observed for ASIP and AgRP, and pharmacological studies revealed AgRP2 is selective for the zebrafish Mc1R. Unlike the human homologue, the zebrafish Mc1R is highly expressed in the brain. Knockdown studies reveal that the AgRP2 protein signals for pigment granule aggregation and is a vital molecule in the background adaptive process. Next, NMR analysis of a β-MSH mutant sequence, identified a tyrosine residue, not involved in receptor binding contacts, that participates in forming a turn motif. Mutation of this residue to cysteine significantly reduces this turn structure and dramatically reduces the agonist binding and activity at Mc4R. This mutation predisposes carriers to early-onset obesity. Finally, we study the non-ICK regions of the AgRP protein. Isothermal titration calorimetry experiments implicate the C-loop in proteoglycan binding and motivated rat feeding studies on C-terminal constructs. Through truncation of this domain, a correlation between peptide charge and appetite stimulation was characterized and led to the design of so-called "Super-AgRP" proteins that stimulate feeding in rodents by more than twice that of wild-type AgRP. These studies have the potential to revolutionize the treatment of cachexia and other negative energy balance metabolic disorders.

Dedication

This work is dedicated to my parents, Gene and Nancy, and my grandmother, Gregoria Molina, for their love and support through this journey, and my brothers, Anthony and Steven, for blazing trails before me. Without you all, this dream could never have been achieved. Thank you.

Acknowledgements:

It has been said that “it takes a village to raise a child”, and in that respect I am no different. It is my extreme privilege to be able to take a moment to acknowledge and honor those people who have helped me reach this incredible achievement.

I would like to thank Dr. Glenn Millhauser for being an incredible advisor and for taking a chance on that young punk so many years ago. He has provided me with an environment to be both productive and creative in the work place and has always been supportive during the highs and lows of graduate studies. I have learned so much during my time in his lab, including how to be a good student and teacher, and without his mentorship I wouldn’t be the scientist I am today.

My coworkers in the Millhauser Lab have also been incredibly helpful and insightful through the many years of my career at UCSC. They have always been there to lend a helping hand, listen to the frustrations of life as a scientist, or provide the well timed and much needed change of subject to areas outside of science. Dr. Pilgrim Jackson and Dr. Darren Thompson recruited me and mentored me in my first year. They taught me the nuances of the melanocortin system and gave me my start in the lab. Dr. Dan Stevens, Dr. Mira Patel, and Dr. Matt Nix were the best officemates I could have. They were always ready for my questions and ready for spirited debate. Dr. Eric Walter, or the Jack-of-all-trades (and master of most), showed me that even the most ancient or intimidating instruments are worth poking around in when they break down and gave me the confidence to solve those problems. And to the next

wave of graduate students in the Millhauser lab, Ann Spevacek, Alex McDonald, Chris Dudzic, and Eric Evans, I consider you all great friends and colleagues and I am confident the lab is in good shape with the four of you at the helm. Just keep the indie-music playing and homebrew's flowing.

I would also like to thank all of the amazing collaborators who have put just as much themselves into these works as I have. Dr. Roger Cone at Vanderbilt University and members of his lab for being ever vigilant with the zebrafish story as well as Dr. Sadaf Farooqi at the Cambridge institute for Medical Research for uncovering the genetics of β-MSH and getting my graduate research off to a cracking start. To Dr. Stephen Benoit and Jennifer Schurdak at the University of Cincinnati I am eternally thankful for their dedication and hard work on the "Super AgRP" work. Their expertise in rodent studies was invaluable and they were great people to work with. I will miss our teleconferences and email discussions.

And lastly, I need to thank all of my friends and family. The road the brought me here has been a long and winding one, and they have always been in my corner cheering me on. Thank you for always being there, I promise to show you all it was worth it.

CHAPTER 1

General Introduction

Cellular Signaling and the Melanocortin System

Vertebrate biology involves a complex array of signaling pathways connecting different tissues and organs to the central nervous system (CNS), allowing the organism to regulate many important physiological processes and adapt to changes in its environment. G-protein coupled receptors (GPCRs) represent the most important receptor type found throughout the body, with over 1000 different types found in the human genome. GPCR's are found in every tissue and have evolved to recognize a wide range of environmental stimuli, from photons and ions to small molecules and proteins, signaling changes in production of the second messenger cAMP, through adenylate cyclase. Because of their prevalence and involvement in virtually every important biological process, GPCRs are the target of more than 50% of the approved pharmaceuticals approved for medical use. The development of such compounds is a remarkable achievement in medicine considering little structural data is available for this super-family of receptors. Until 2007, the only available crystal structure of a eukaryotic GPCR was that of rhodopsin, the photoreceptor expressed in the retina and responsible for vision. This structure served as the basis for subsequent GPCR modeling.

The melanocortin receptors, a subset of the GPCR family, and their ligands, regulate some of the most vital physiological processes including: pigmentation, coat color, inflammatory response, steroidogenesis, sexual behavior, and energy balance and homeostasis (*1*, *2*). McRs are activated by

small peptides derived from the proopiomelanocortin (POMC), resulting in an increase in production of cAMP. Unlike other GPCR signaling pathways, the melanocortin system also possesses an additional layer or regulation with the presence of endogenous antagonists (*3*). These antagonists compete with POMC derived ligands at specific McRs, preventing cAMP stimulation. This provides the McR system with an additional set of tools to probe receptor activity and aids in the development of therapeutics.

It has become increasingly important to understand this system due to its link to metabolic disorders. In the US, obesity has become a critical health issue. According to the Centers for Disease Control and Prevention (CDC), nearly 36% of American adults and 17% of children suffer from obesity (≥30BMI). Similarly, chronic diseases like heart disease, cancer and AIDS, result in dramatically increasing numbers of people suffering from the negative energy balance syndrome cachexia (*4*, *5*). Studies have shown melanocortins in the CNS directly contribute to these disorders, however little progress has been made in the development of treatments (*6*). Because of this, continued efforts into understanding ligand and receptor determinants remains of utmost importance.

Melanocortin Receptors

There are five different melanocortin receptors (Mc1R-Mc5R), with each receptor displaying a unique set of tissue expression and ligand binding

specificity (Figure 1) (*7*). The works presented here focuses on the hypothalamic receptors Mc3R and Mc4R, but also investigates a specific interaction at Mc1R in teleost fish. Like all GPCRs, they are expressed as a single chain, containing 7 transmembrane helices. Ligand binding events occur in the extracellular side of the membrane, with the G-protein coupling to intracellular loops of the receptor. When activated by agonist ligands, McRs release a stimulatory Gα subunit that causes synthesis of the second messenger cAMP through adenylate cyclase. In addition to detailed regulation by competitive ligands, the melanocortin receptors are also constitutively active, producing a basal level of cAMP, creating a highly unique competitive/constitutive environment.

Mc1R was the first discovered McR, and is primarily expressed in skin melanocytes, although it is also expressed in some immune-response cells lines and in the hypothalamus of some lower vertebrates. There, Mc1R helps regulate skin pigmentation and coat color in mammals through interactions with agonists derived from proopiomelanocortin (POMC) and the endogenous antagonist agouti-signaling protein (ASIP) (*8*). Agonist signaling results in eumelanin, or brown pigment production whereas antagonist activity signals for pheomelanin, or yellow pigment is produced. This has been extensively studied in mice. Biosynthesis of ASIP is temporally regulated in wild type mice producing hair with dark/yellow/dark patterning. Overexpression of ASIP prevents agonist signaling and produces a full yellow coat.

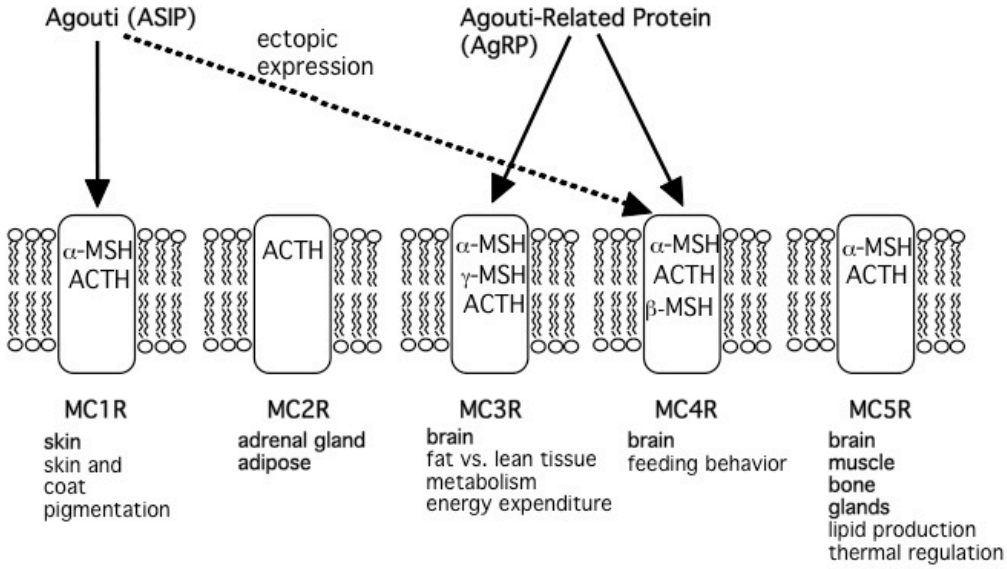

Figure 1. Diagram depicting the current understanding of the melanocortin system. Agonists are shown inside the receptors they bind to, with antagonists shown above. Dashed arrow indicates a non-native interaction.

Mc3R and Mc4R are centrally expressed in specific neurons of the hypothalamus and are directly involved in energy balance and homeostasis. Mc3R shows roughly equal affinity for the POMC derived agonists α, β, and γ-MSH, while Mc4R only exhibits affinity for α and β-MSH (*9*). Activation of these receptors signals for increased energy expenditure, anorexic behavior, and lean body mass. These receptors are also antagonized by both endogenous antagonists, agouti-signaling and agouti-related proteins (ASIP and AgRP). Antagonist signaling through Mc3/4R produces orexigenic behavior and decreased energy expenditure. Mice lacking a functional Mc3R exhibit a roughly 50% increase in adipose mass and decreased energy expenditure (*10*, *11*). Mc4R knockout mice are severely obese, hyperphagic, and exhibit symptoms similar to type-II diabetes such as hyperinsulinemia (*12*, *13*).

Melanocortin Agonists

The agonists of the melanocortin receptors are derived from the 241 residue prohormone POMC. This protein is expressed in many different tissues throughout the body including the skin, corticotrophs, the lymphoid system, and POMC-neurons in the arcuate nucleus of the hypothalamus (*14*). Once excreted, POMC is processed by prohormone convertases to release specific McR agonist ligands (*15*). Outside of the CNS, prohormone convertase 1 (PC1) cleavage produces N-terminal peptide (NT), joining

peptide (JP), adrenocorticotropin (ACTH) and β-lipotropin (β-LP). Within the hypothalamus, PC2 expression produces α, β, and γ-melanocyte stimulating hormones (MSH) and β-endorphin (Figure 2). PC1/2 act at specific dibasic sites found within the prohormone, and not all site are conserved across species. For example, rodents lack the PC2 recognition site to release β-MSH.

Mutations preventing POMC synthesis or processing, cause obesity and pigmentation disorders (*16*). Because of this, a great amount of effort has gone into understanding the key features of agonist activity. ACTH and all three MSH peptides exhibit McR binding affinity. These melanocortin agonists are small, unstructured peptides, ranging in length from 11-39 amino acids, containing the consensus HFRW sequence (*17*). Pharmacological studies have demonstrated that this quartet represents the required motif for high affinity agonist activity at melanocortin receptors. Attempts at creating synthetic analogues to these endogenous agonists using the HFRW sequence have produced MSH mimetics that induce melanogenesis (tanning) of skin cells but with side effects on sexual function due to lack of receptor specificity.

Melanocortin Antagonists

The melanocortin system is unique in the GPCR super family is that it also contains endogenous antagonists. Agouti-signaling protein (ASIP) and

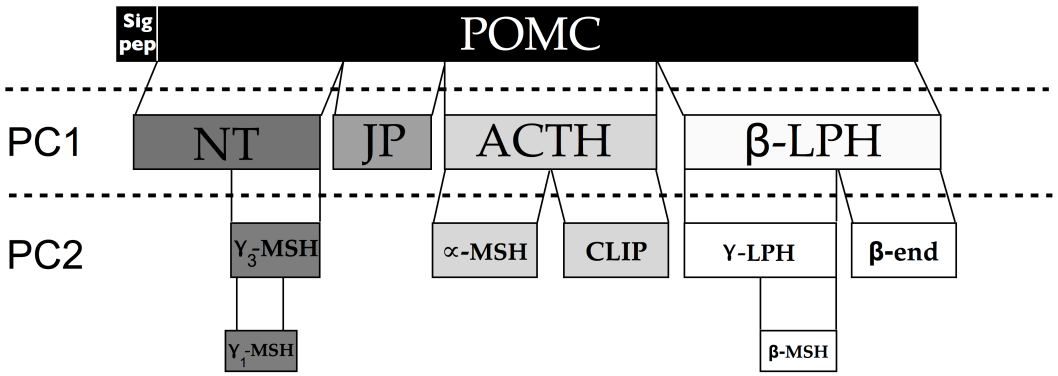

Figure 2. Diagram of the proopiomelanocortin (POMC) expression product (top) and subsequent post-translational processing by prohormone convertase 1 (middle) and prohormone convertase 2 (bottom)

agouti-related protein (AgRP) display the remarkable ability to compete against POMC agonists for receptor binding, and even exhibit inverse-agonist activity by reducing constitutive cAMP production (*18*, *19*). ASIP is normally expressed in the skin where is interacts with Mc1R to stimulate the production of pheomelanin, however a specific mouse genetic mutation can cause ectopic expression of ASIP and results in a severely obese phenotype with full yellow coat (*20*). The non-pigment related effects of this mutation were later found to be caused by interactions of ASIP at Mc3R and Mc4R in the CNS. This development led to the search for an ASIP homologue expressed in the brain and the discovery of AgRP(*21*).

Structurally, ASIP and AgRP are very similar. They are expressed as approximately 132aa proteins with a 20aa signaling sequence(*22*). The first 60 residues form an unstructured N-terminal domain. The final 50aa contains 10 cysteine residues that fully oxidize to form 5 disulfide bonds and produce a structured C-terminal domain composed of three loops, as determined by NMR (*23*). The first three disulfide bridges form an inhibitor cystine knot (ICK) fold (*24-26*). This structural motif is commonly found in toxins of marine cone snails, scorpions and spiders, however ASIP and AgRP represent the only known mammalian proteins with this fold. Virtually all of the sequence homology between ASIP and AgRP is found in the C-terminal domain, producing protein folds that are virtually superimposable (Figure 3), yet AgRP

displays no affinity for Mc1R. This receptor selectivity has motivated extensive studied into structural determinants for receptor binding.

Owning to a lack of structural data for melanocortin receptors, researchers have had to rely on receptor mutagenesis and synthetic proteins to elucidate the key features of antagonism. Pharmacological studies have identified the middle loop as the putative “active-loop”. Alanine scanning through this region has singled out the Arg-Phe-Phe triplet, which projects out from the top of this loop, as absolutely essential for receptor activity (*27*-*29*). This loop is not sufficient to provide high affinity binding however. A minimized AgRP construct (miniAgRP) designed with first, or “N-terminal loop”, along with the active-loop, completely restores high affinity binding at Mc3R and Mc4R (*30*). Attempts to design a similar minimized ASIP construct produced variants with high affinity binding to Mc1R, but with agonist activity. Together, these results indicate that the first two loops of ASIP and AgRP contain the required receptor contacts for high-affinity binding. Additionally, the third or “C-terminal” loop of ASIP conveys antagonist activity at Mc1R, however no discernable physiological function has previously been elucidated for the C-loop of AgRP (*31*).

The unstructured N-terminal domain of ASIP is required for full activity *in vivo* (*32*). Experiments on transgenic mice have shown a possible interaction between this domain and the membrane-bound glycoprotein attractin. Mice lacking a functional attractin gene exhibit an extreme agonist,

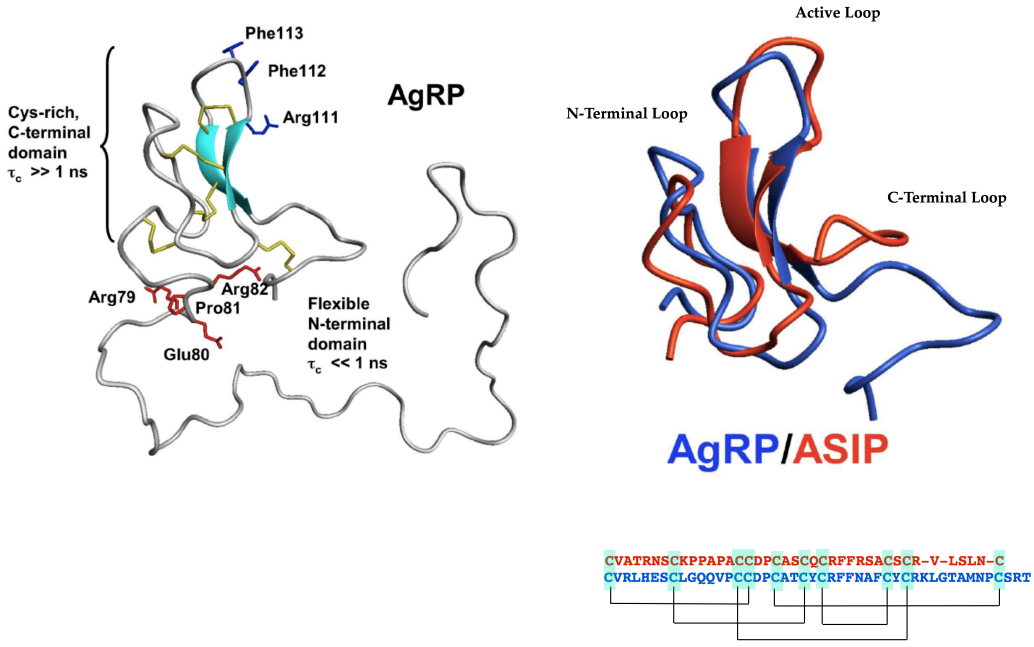

Figure 3. *Left*- Model of full-length AgRP illustrating the flexible N-terminal domain and key features of the C-terminal domain, including disulfide bridges and the essential RFF triplet. *Right*- Solution NMR structures of the C-terminal domains of ASIP (red) and AgRP (blue), showing the near super-imposability. Sequence alignment shows the specific disulfide connectivity. (*33*)

or dark coat phenotype. Furthermore, binding studies show that attractin displays a dissociation constant of 0.7mM for the unstructured region of ASIP, but no affinity for either the C-terminal domain of ASIP. Analysis of vertebrate ASIP sequences reveals patches of high sequence conservation, particularly in mammalian species. AgRP, on the other hand, shows little sequence conservation in the region preceding the Cys-rich domain (*33*).

It has been proposed that AgRP interacts with syndecan-3, a heperin sulfate proteoglycan (HSPG) expressed in the hypothalamus (*34*). Mice studies show up regulation of syndecan-3 expression at Mc3/4R neurons during periods of food deprivation. Transgenic mice expressing syndecan-1, a persistent homologue to syndecan-3, also exhibit markedly increased linear growth. Similarly, HEK293 cells co-expressing syndecans with Mc4R all show increased AgRP activity. These results display a striking similarity to those observed for the activity of ASIP at Mc1R and its mediation by attractin. Despite this, no physical binding interaction has been resolved for the N-terminal domain of AgRP and syndecans. This theory has been further complicated by new studies demonstrating that the unstructured domain acts as a prodomain, reducing AgRP activity *in vivo* (*35*, *36*). The full-length protein exhibits a 10-fold weaker dissociation constant and EC_{50} value for Mc4R activity than that observed for the C-terminal peptide $AgRP_{83-132}$. Furthermore, *in vivo* studies indicate the flexible region is removed through

proteolytic cleavage by proprotein convertases immediately following a dibasic recognition site at Arg81-Arg82.

Thesis Outline

With its connection to key human health issues, the hypothalamic melanocortin system is positioned as a prime target for potential therapeutics of metabolic disorders. Efforts in this area have been ongoing and have produced significant advances in the understanding of receptor binding determinants in the absence of a fully resolved receptor structure. Despite these advances, a number of important details of this signaling pathway remain unresolved. A functional significance for the C-terminal loop of AgRP has yet to be elucidated and the specifics of a possible AgRP/syndecan binding interaction remain a mystery. Likewise, ongoing genetic studies continue to reveal new melanocortin ligands, in humans and lower vertebrates, with uncharacterized structural and physiological properties (*37*).

The research presented here addresses three main areas of interest. Chapter 2 is a rewritten manuscript by Chao Zhang from the laboratory of Roger Cone, studying the physiological significance of a novel, third antagonist sequence (AgRP2) discovered in teleost fish (*38*). Chapter 3 emphasizes my efforts in the study of structural changes of the mutant agonist β-MSH Tyr221Cys that affect receptor activity (*39*). Chapters 4 and 5 investigate the physiological role of the non-ICK regions of the agouti-related

protein. Chapter 4 composes isothermal titration calorimetry (ITC) experiments on recombinant and synthetic AgRP sequences, including the N-terminal domain, and is written in manuscript format. Motivated by the ITC experiments, Chapter 5 studies the effects of eight C-terminal AgRP constructs on feeding behavior in rats, and is a reprint of the manuscript submitted to ACS Chemical Biology (*40*). Through these experiments a physiological significance to regions not involved in receptor binding has been uncovered that has the potential to provide significant advances in pharmaceutical therapeutics for metabolic disorders.

References

1. Tatro, J. B. (1996) Receptor biology of the melanocortins, a family of neuroimmunomodulatory peptides, *Neuroimmunomodulation 3*, 259–284.
2. Gantz, I., and Fong, T. M. (2003) The melanocortin system, *Am J Physiol Endocrinol Metab 284*, E468–74.
3. Abdel-Malek, Z. A. (2001) Melanocortin receptors: their functions and regulation by physiological agonists and antagonists, *Cell Mol Life Sci 58*, 434–441.
4. Tan, B. H. L., and Fearon, K. C. H. (2008) Cachexia: prevalence and impact in medicine, *Curr Opin Clin Nutr Metab Care 11*, 400–407.
5. Haehling, von, S., Lainscak, M., Springer, J., and Anker, S. D. (2009) Cardiac cachexia: a systematic overview, *Pharmacol Ther 121*, 227–252.
6. Scarlett, J. M., Bowe, D. D., Zhu, X., Batra, A. K., Grant, W. F., and Marks, D. L. (2010) Genetic and pharmacologic blockade of central melanocortin signaling attenuates cardiac cachexia in rodent models of heart failure, *J Endocrinol 206*, 121–130.
7. Chhajlani, V. (1996) Distribution of cDNA for melanocortin receptor subtypes in human tissues., *Biochem. Mol. Biol. Int. 38*, 73–80.
8. Millar, S. E., Miller, M. W., Stevens, M. E., and Barsh, G. S. (1995) Expression and transgenic studies of the mouse agouti gene provide insight into the mechanisms by which mammalian coat color patterns are generated., *Development 121*, 3223–3232.
9. Abbott, C. R., Rossi, M., Kim, M., AlAhmed, S. H., Taylor, G. M., Ghatei, M. A., Smith, D. M., and Bloom, S. R. (2000) Investigation of the melanocyte stimulating hormones on food intake. Lack Of evidence to support a role for the melanocortin-3-receptor., *Brain Res 869*, 203–210.
10. Chen, A. S., Marsh, D. J., Trumbauer, M. E., Frazier, E. G., Guan, X. M., Yu, H., Rosenblum, C. I., Vongs, A., Feng, Y., Cao, L., Metzger, J. M., Strack, A. M., Camacho, R. E., Mellin, T. N., Nunes, C. N., Min, W., Fisher, J., Gopal-Truter, S., MacIntyre, D. E., Chen, H. Y., and van der Ploeg, L. H. (2000) Inactivation of the mouse melanocortin-3 receptor results in increased fat mass and reduced lean body mass., *Nat Genet 26*, 97–102.
11. Butler, A. A., Kesterson, R. A., Khong, K., Cullen, M. J., Pelleymounter, M. A., Dekoning, J., Baetscher, M., and Cone, R. D. (2000) A unique metabolic syndrome causes obesity in the melanocortin-3 receptor-deficient mouse., *Endocrinology 141*, 3518–3521.
12. Huszar, D., Lynch, C. A., Fairchild-Huntress, V., Dunmore, J. H., Fang, Q., Berkemeier, L. R., Gu, W., Kesterson, R. A., Boston, B. A., Cone, R. D., Smith, F. J., Campfield, L. A., Burn, P., and Lee, F. (1997) Targeted

disruption of the melanocortin-4 receptor results in obesity in mice, *Cell 88*, 131–141.
13. Vaisse, C., Clement, K., Durand, E., Hercberg, S., Guy-Grand, B., and Froguel, P. (2000) Melanocortin-4 receptor mutations are a frequent and heterogeneous cause of morbid obesity., *J Clin Invest 106*, 253–262.
14. Hadley, M. E., and Haskell-Luevano, C. (1999) The proopiomelanocortin system, *Ann N Y Acad Sci 885*, 1–21.
15. Seidah, N. G., and Chrétien, M. (1999) Proprotein and prohormone convertases: a family of subtilases generating diverse bioactive polypeptides, *Brain Res 848*, 45–62.
16. Pritchard, L. E., Turnbull, A. V., and White, A. (2002) Pro-opiomelanocortin processing in the hypothalamus: impact on melanocortin signalling and obesity., *J Endocrinol 172*, 411–421.
17. Bednarek, M. A., Silva, M. V., Arison, B., MacNeil, T., Kalyani, R. N., Huang, R.-R. C., and Weinberg, D. H. (1999) Structure-function studies on the cyclic peptide MT-II, lactam derivative of α-melanotropin, *Peptides 20*, 401–409.
18. Srinivasan, S., Lubrano-Berthelier, C., Govaerts, C., Picard, F., Santiago, P., Conklin, B. R., and Vaisse, C. (2004) Constitutive activity of the melanocortin-4 receptor is maintained by its N-terminal domain and plays a role in energy homeostasis in humans, *J Clin Invest 114*, 1158–1164.
19. Haskell-Luevano, C., and Monck, E. K. (2001) Agouti-related protein functions as an inverse agonist at a constitutively active brain melanocortin-4 receptor., *Regul. Pept. 99*, 1–7.
20. Lu, D., Willard, D., Patel, I. R., Kadwell, S., Overton, L., Kost, T., Luther, M., Chen, W., Woychik, R. P., Wilkison, W. O., and Cone, R. D. (1994) Agouti protein is an antagonist of the melanocyte-stimulating-hormone receptor, Nature Publishing Group *371*, 799–802.
21. Ollmann, M. M., Wilson, B. D., Yang, Y. K., Kerns, J. A., Chen, Y., Gantz, I., and Barsh, G. S. (1997) Antagonism of central melanocortin receptors *in vitro* and *in vivo* by agouti-related protein., *Science 278*, 135–138.
22. Willard, D. H., Bodnar, W., Harris, C., Kiefer, L., Nichols, J. S., Blanchard, S., Hoffman, C., Moyer, M., Burkhart, W., and Weiel, J. (1995) Agouti structure and function: characterization of a potent alpha-melanocyte stimulating hormone receptor antagonist, *Biochemistry 34*, 12341–12346.
23. Rossi, M., Kim, M. S., Morgan, D. G., Small, C. J., Edwards, C. M., Sunter, D., Abusnana, S., Goldstone, A. P., Russell, S. H., Stanley, S. A., Smith, D. M., Yagaloff, K., Ghatei, M. A., and Bloom, S. R. (1998) A C-terminal fragment of Agouti-related protein increases feeding and antagonizes the effect of alpha-melanocyte stimulating hormone *in vivo*,

Endocrinology 139, 4428–4431.
24. McNulty, J. C., Jackson, P. J., Thompson, D. A., Chai, B., Gantz, I., Barsh, G. S., Dawson, P. E., and Millhauser, G. L. (2005) Structures of the agouti signaling protein, *J Mol Biol 346*, 1059–1070.
25. McNulty, J. C., Thompson, D. A., Bolin, K. A., Wilken, J., Barsh, G. S., and Millhauser, G. L. (2001) High-resolution NMR structure of the chemically-synthesized melanocortin receptor binding domain AGRP(87-132) of the agouti-related protein, *Biochemistry 40*, 15520–15527.
26. Yu, B., and Millhauser, G. L. (2007) Chemical disulfide mapping identifies an inhibitor cystine knot in the agouti signaling protein., *FEBS Lett 581*, 5561–5565.
27. Kiefer, L. L., Veal, J. M., Mountjoy, K. G., and Wilkison, W. O. (1998) Melanocortin receptor binding determinants in the agouti protein., *Biochemistry 37*, 991–997.
28. Kiefer, L. L., Ittoop, O. R., Bunce, K., Truesdale, A. T., Willard, D. H., Nichols, J. S., Blanchard, S. G., Mountjoy, K., Chen, W. J., and Wilkison, W. O. (1997) Mutations in the carboxyl terminus of the agouti protein decrease agouti inhibition of ligand binding to the melanocortin receptors., *Biochemistry 36*, 2084–2090.
29. Haskell-Luevano, C., Monck, E. K., Wan, Y. P., and Schentrup, A. M. (2000) The agouti-related protein decapeptide (Yc[CRFFNAFC]Y) possesses agonist activity at the murine melanocortin-1 receptor, *Peptides 21*, 683–689.
30. Jackson, P. J., McNulty, J. C., Yang, Y.-K., Thompson, D. A., Chai, B., Gantz, I., Barsh, G. S., and Millhauser, G. L. (2002) Design, pharmacology, and NMR structure of a minimized cystine knot with agouti-related protein activity, *Biochemistry 41*, 7565–7572.
31. Patel, M. P., Cribb Fabersunne, C. S., Yang, Y.-K., Kaelin, C. B., Barsh, G. S., and Millhauser, G. L. (2010) Loop-swapped chimeras of the agouti-related protein and the agouti signaling protein identify contacts required for melanocortin 1 receptor selectivity and antagonism., *J Mol Biol 404*, 45–55.
32. He, L., Gunn, T. M., Bouley, D. M., Lu, X. Y., Watson, S. J., Schlossman, S. F., Duke-Cohan, J. S., and Barsh, G. S. (2001) A biochemical function for attractin in agouti-induced pigmentation and obesity, *Nat Genet 27*, 40–47.
33. Jackson, P. J., Douglas, N. R., Chai, B., Binkley, J., Sidow, A., Barsh, G. S., and Millhauser, G. L. (2006) Structural and molecular evolutionary analysis of Agouti and Agouti-related proteins., *Chem. Biol. 13*, 1297–1305.
34. Reizes, O., Lincecum, J., Wang, Z., Goldberger, O., Huang, L., Kaksonen, M., Ahima, R., Hinkes, M. T., Barsh, G. S., Rauvala, H., and Bernfield, M. (2001) Transgenic expression of syndecan-1 uncovers a

physiological control of feeding behavior by syndecan-3, *Cell 106*, 105–116.
35. Creemers, J. W. M., Pritchard, L. E., Gyte, A., Le Rouzic, P., Meulemans, S., Wardlaw, S. L., Zhu, X., Steiner, D. F., Davies, N., Armstrong, D., Lawrence, C. B., Luckman, S. M., Schmitz, C. A., Davies, R. A., Brennand, J. C., and White, A. (2006) Agouti-related protein is posttranslationally cleaved by proprotein convertase 1 to generate agouti-related protein (AGRP)83-132: interaction between AGRP83-132 and melanocortin receptors cannot be influenced by syndecan-3., *Endocrinology 147*, 1621–1631.
36. Pritchard, L. E., and White, A. (2005) Agouti-related protein: more than a melanocortin-4 receptor antagonist?, *Peptides 26*, 1759–1770.
37. Kurokawa, T., Murashita, K., and Uji, S. (2006) Characterization and tissue distribution of multiple agouti-family genes in pufferfish, Takifugu rubripes, *Peptides 27*, 3165–3175.
38. Zhang, C., Song, Y., Thompson, D. A., Madonna, M. A., Millhauser, G. L., Toro, S., Varga, Z., Westerfield, M., Gamse, J., Chen, W., and Cone, R. D. (2010) Pineal-specific agouti protein regulates teleost background adaptation., *Proc Natl Acad Sci USA 107*, 20164–20171.
39. Lee, Y. S., Challis, B. G., Thompson, D. A., Yeo, G. S. H., Keogh, J. M., Madonna, M. E., Wraight, V., Sims, M., Vatin, V., Meyre, D., Shield, J., Burren, C., Ibrahim, Z., Cheetham, T., Swift, P., Blackwood, A., Hung, C.-C. C., Wareham, N. J., Froguel, P., Millhauser, G. L., O'Rahilly, S., and Farooqi, I. S. (2006) A POMC variant implicates beta-melanocyte-stimulating hormone in the control of human energy balance, *Cell Metab 3*, 135–140.
40. Madonna, M. E., Schurdak, J., Yang, Y.-K., Benoit, S., and Millhauser, G. L. (2012) Agouti-Related Protein Segments Outside of the Receptor Binding Core Are Required for Enhanced Short- and Long-term Feeding Stimulation., *ACS Chem. Biol. 7*, 395–402.

CHAPTER 2

(Zebrafish AgRP2)

Synthesis and characterization of a novel third antagonist sequence, AgRP2, in Zebrafish

(Much of the text and figures of this chapter appeared originally as “Pineal-specific agouti protein regulates teleost background adaptation.” Submitted to PNAS. The work was done in collaboration with the Roger Cone laboratory at the University of Oregon (now at Vanderbilt) and is reprinted with permission. My role in this project involved the synthesis, oxidative folding, and purification of zebrafish AgRP2 for pharmacological characterization.)

Abstract

Background adaptation is used teleosts to provide camouflage and avoid predation. This pigmentation change is accomplished through various pathways and is known to involve light sensing mechanisms, signaling for contraction or dispersion of pigment granules. Here we demonstrate the synthesis of an agouti gene unique to teleosts, AgRP2, from its genetic sequence, and subsequent receptor pharmacology and expression profile. This protein is explicitly produced in the pineal and regulates expression of melanocyte concentrating hormone (MCH) and MCH-like (MCHL) genes through interactions at melanocortin 1 receptor (Mc1R) in the hypothalamus. These studies elucidate a role for the pineal in background adaptation of teleosts and represent a unique function for agouti-related antagonist whereby environmental stimuli affect melanocortin signaling.

Introduction

Pigmentation signaling is a vital process for all vertebrates. In mammals, the up-regulation of different pigment molecules affects animal coat color, which is essential for animal camouflage. This is a slow process, requiring shedding of the previous coat and growth of the new hair. By contrast, lower vertebrates like reptiles, amphibians and teleost fish, are able to rapidly change skin pigmentation at the cellular level in order to adapt to their surroundings.

In all vertebrates, this process is partially regulated through ligand binding events at the G-protein coupled Melanocortin 1 receptor (MC1r) in the skin (*1*). Interaction with the endogenous agonist, α-Melanocyte stimulating hormone (α-MSH), results in an increase of cAMP. This second messenger causes several downfield reactions, including an increase in eumelanin production in mammals and pigment granule dispersion in lower vertebrates. In both cases, this causes a dark phenotype. The agouti-signaling peptide (ASIP) is an endogenous antagonist of α-MSH at MC1r. This protein causes a reduction in cellular cAMP levels, which up-regulates pheomelanin synthesis in mammals and pigment granule aggregation in lower vertebrates (*2*). The result of ASIP signaling is a light color phenotype.

The interactions of melanocortins in the skin can explain the standard pigmentation phenotype in vertebrates, however it cannot describe background adaptation in animals. It has long been understood that there is a

link between photo-sensing regions in the brain and pigmentation changes (*3*). Mammals receive photic input from the retina, where the signal is connected to the CNS. By contrast, non-mammalian vertebrates contain a variety of opsin receptors in the pineal gland of the brain and can receive photic input into the CNS directly (*4*, *5*). This light-sensitive part of the brain has been shown to project to the hypothalamus where it plays a vital role in the diurnal cycle.

The pineal gland has long been implicated in the background adaptation of teleost fish. Direct exposure of the pineal to light causes hypothalamic increase in melanin-concentrating hormone (MCH) pigment granule aggregation, whereas covering the pineal with India ink stimulates a-MSH synthesis and pigment dispersion (*6*, *7*). The link between the pineal and hypothalamus implicates the melanocortin system in pigment switching for teleost fish (*8*, *9*). The hypothalamic melanocortin receptors Mc3R and Mc4R have been well studied for their effects on energy balance and homeostasis(*10*). Similar to Mc1R in the skin, these GPCRs are agonized by α-MSH and antagonized by the ASIP homologue Agouti-related protein (AgRP).

Through the complete sequencing of the zebrafish genome, a third agouti-like gene has recently been discovered, *agrp2* (*11*). Figure 1 shows sequence alignments for all three zebrafish agouti proteins with the human counter parts. The cysteine-rich C-terminal domain of human ASIP and AgRP

```
hASIP    CVATRNSCKPPAPACCDPCASCQCRFFRSACSCR-V-LSLN-C
zASIP    CVPLWASCKSPNAVCCDQCAFCHCRLLKTVCYCR-MGY--PKC
hAgRP    CVRLHESCLGQQVPCCDPCATCYCRFFNAFCYCRKLGTAMNPCSRT
zAgRP    CIPHQQSCLGHHLPCCNPCDTCYCRFFKAFCYCRSMD---NTCKNEYA
zAgRP2   CAGLTESC-SSLTPCCDPCASCHCRLFNTICHCWRLGH-L--CPKKT
```

Figure 1. (Above) Alignment of melanocortin antagonist sequences from human and zebrafish genomes. (Below) Structural similarity of hASIP (red), hAgRP (blue), and a model of zAgRP2 (green). AgRP2 structure was generated using the Modeler 9v8 software package using the human AgRP structure as the beginning conformation.

contains the necessary contacts for high-affinity receptor binding *in vitro* (*12*). Within this domain, zAgRP2 displays 43% sequence identity with hASIP and 50% identity with hAgRP, including conservation of all 10 cysteines and RXF receptor binding motif. As such, this new AgRP sequence should exhibit similar pharmacology at melanocortin receptors. The C-terminal domain of agouti peptides is well within the limits of solid-phase peptide synthesis. Previous work by the Millhauser lab has fully described the synthesis and folding conditions for the human variants and as such, made this method amenable for study of zAgRP2 (*13*). While synthesis yields are far below that commonly expected of a fully optimized expression system, the quantity obtained is easily sufficient to facilitate standard pharmacological studies and can be generated within a three weeks, from start to finish.

The focus of this research was to chemically synthesize the C-terminal domain of zAgRP2, form all five disulfide bonds via oxidative folding, and fully characterize its melanocortin receptor pharmacology. Through collaborative efforts with my colleague, Darren Thompson, and the Cone lab at the University of Oregon (now at Vanderbilt), we also characterized the pharmacology of zAgRP as well as studied the *in vivo* function of zAgRP2. These studies describe a physiological role for this new AgRP sequence in environmental background adaptation. Furthermore, this represents a completely new pathway by which the pineal and hypothalamus regulate pigmentation.

Methods

Peptide Synthesis & Purification

Zebrafish AgRP (Ac-83-127-NH3) and AgRP2 (Ac-Y-83-127-NH3) were synthesized using Fmoc synthesis on an Applied Biosystems 433A Peptide Synthesizer on a 0.25-mmol scale and monitored using the SynthAssist 2.0 software package. All peptides were assembled on a Rink-amide-4-methyl- benzhydrylamine resin, and preactivated Fmoc-Cys(trt)-OPfp was used. All amino acids and resins were purchased through Nova-Biochem. HBTU 2-(1H-benzotriazole-1-yl)-1,1,3,3-tetramethyluronium hexafluorophosphate (HBTU) was obtained from Advanced Chemtech, and all other reagents were purchased from Sigma- Aldrich. Fmoc deprotection was achieved using a 1% hexamethyleneimine (HMI) and 1% 1,8-diazabicyclo[4.5.0]-undec-7-ene (DBU) solution in dimethyl formamide (DMF). Deprotection was monitored by conductivity and continued until the conductivity level returned to the baseline, then synthesis continued. Deprotection time ranged from 2.5 to 7 min. Coupling used four equivalents Fmoc- amino acid in HBTU/N,N-Diisopropylethylamine (DIEA) for all amino acids except the preactivated cysteine. A threefold excess of Fmoc-Cys(trt)-OPfp was dissolved in 1.5 mL 0.5 M 1-Hydroxy-7-azabenzotriazole/DMF with no DIEA for coupling. The peptides were N-terminal acetylated by reacting with 0.5 M acetic anhydride in DMF for 5 min. A tyrosine residue was added to the N-terminal end of zebrafish AgRP2 for ^{125}I radiolabeling. Fully

synthesized peptide resins were split into three reaction vessels, washed with di- chloromethane, and dried. A solution of 8 mL TFA containing 200 µL each of triisopropylsilane/1,2-ethanedithiol/liquefied Phenol (as scavengers) was added to each reaction vessel of dry peptide resin for 1.5 h. The resin was filtered and washed with 1 mL TFA, and the combined filtrate and wash was then added to 90 mL cold dry diethyl ether for precipitation. The precipitate was collected by centrifugation, and the ether was discarded. The pellet was dis- solved in 40 mL 1:1 H2O:ACN (0.1% TFA) and lyophilized. Peptide purification was achieved by RP-HPLC on Vydac preparative columns (C4 for AgRP and C18 for AgRP2). Fractions were collected and analyzed by ESI-MS on a Micromass ZMD mass spectrometer to confirm the correct molecular weight. In each case the major peak was found to be the peptide, and fractions, which contained the peptide as a major constituent, were combined and lyophilized.

Oxidative Folding

Air oxidative folding of zebrafish AgRP was accomplished by dissolving the unfolded peptide into folding buffer (2.0 M GuHCl/0.1 M Tris, 3 mM reduced glutathione, 400 µM oxidized glutathione, pH 8) at a peptide concentration of 0.1 mg/mL) and stirring for 14 h. Oxidative folding by DMSO of zebrafish AgRP2 was done by dissolving the unfolded peptide into the folding buffer with 5% DMSO and a peptide concentration of 1 mg/mL and stirring for 4 h.

Folding was monitored for both peptides by RP- HPLC on a C18 analytical column, which revealed a single peak, in each case, for the folded material that was shifted to an earlier retention time than the fully reduced peptide. The folded product was purified by RP-HPLC on a C18 preparative column and its identity confirmed as the fully oxidized product by ESI-MS (AgRP Ac-83-127-NH2: 5287.1 calc. ave. isotopes 5288 amu obs.; AgRP2 Ac-Y-94-136-NH2 4894.8 calc. ave. isotopes 4896 amu obs.).

Receptor Pharmacology

Zebrafish melanocortin receptor 1 was amplified from skin cDNA according to the published sequences. PCR products were subcloned into the pcDNA3.1+ vector using BamH I and EcoR I sites. Zebrafish melanocortin receptor 3 was kindly provided by Dr. Darren Logan (Western General Hospital, Edinburgh, United Kingdom). pGEMT-zMC3R was digested by Not I enzyme and subcloned into pcDNA3.1+ using the same restriction site. Zebrafish melanocortin receptor 4, 5a, and 5b were independently cloned from a zebrafish brain cDNA library. Zebrafish melanocortin receptor 4 and 5a were subcloned into pcDNA3.1+ using a BamH I site, and zebrafish melanocortin receptor 5b was cloned into pcDNA3.1+ using a Not I site. Stable transfectants were made in HEK-293 cells using lipofectamine or lipofectamine2000 (Invitrogen), followed by selection in 1,000 μg/mL G418.

Zebrafish melanocortin receptor activity was measured using a cAMP-dependent β-galactosidase assay in HEK-293 cell transfectants as described previously (*50*). Cells were incubated with serially diluted concentrations of α-MSH in the presence or absence of zAgRP(83–127) or zAgRP2(93-136) in a final 50-μL volume using a 96-well format. Color development was measured at 405 nm with a Benchmark Plus plate spectrophotometer (Bio-Rad).

Results and Discussion

Peptide Synthesis & Oxidative Folding

The new agouti sequence, zAgRP2, was generated by solid-phase peptide synthesis on an ABI 433A peptide synthesizer, using standard Fmoc chemistry. An N-terminal tyrosine was added to the sequence for UV identification and to allow for the potential to radiolabel the ligand at a future date. The fully synthesized product was removed from the resin via cleavage by trifluoroacetic acid (TFA). HPLC analysis of the crude product revealed the full protein as the major peak, with a tert-butyl addition as secondary product. Impurities were removed by further RP-HPLC purification on a Vydac C4 preparatory column. ESI-Mass Spectrometry identified fractions containing the appropriate product, with a mass of 4906amu. After lyophilization, approximately 100mg of dried, unfolded peptide was obtained.

To form the five native disulfide bonds, the purified peptide was dissolved in folding buffer to a concentration of 0.1mg/1.0mL. At this concentration the peptide is less likely to form intra-molecular disulfide bridges or aggregates. The solution was allowed to air-oxidize and folding was monitored by RP-HPLC. Figure 2 shows four time points in the folding process: t = 0, t = 1.5 hours, t = 4.5hr, and t = 24hr. Within the first 90min a significant portion of the peptide has folded, as identified by a shift to a lower retention time. It is possible that this fold does not represent the native fold, so the peptide was allowed to continue until the initial t = 0 peak disappeared.

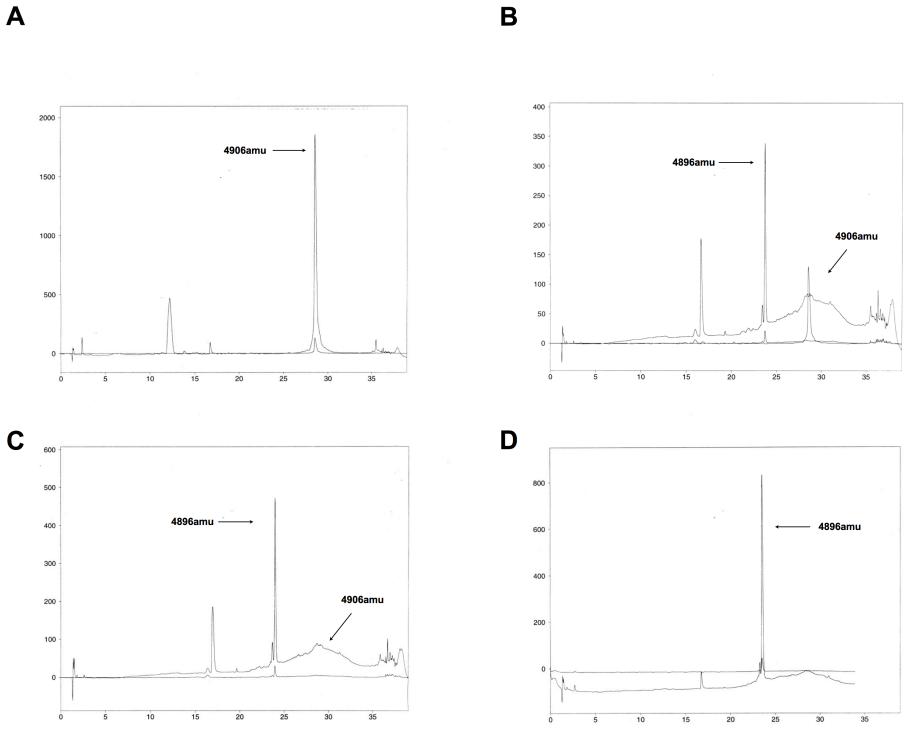

Figure 2. Oxidative folding of synthetic zebrafish AgRP2. HPLC chromatograms of time points t=0 (A), t=1.5hr (B), t=4.5hr (C), and t=24hr (D). Formation of disulfide bonds causes a shift to a lower retention time. Corresponding mass spectrometry data for t=0 and t=24hr are shown within the chromatogram.

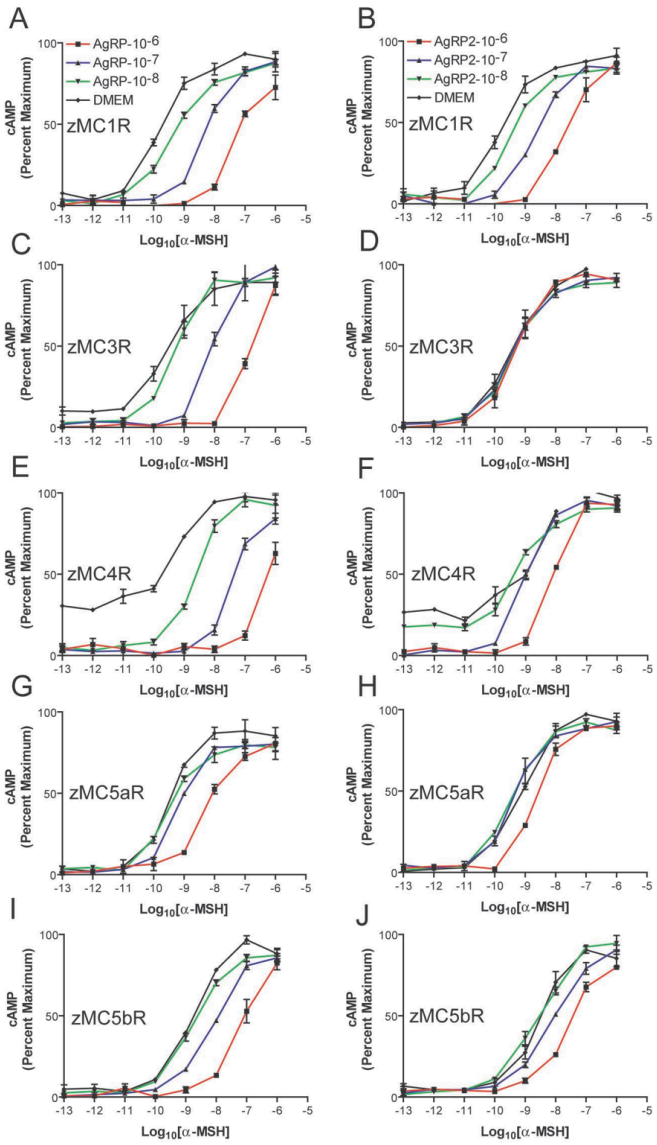

Figure 3. Pharmacological activity of zebrafish AgRP(83–127) and AgRP2(93–136) peptides. The left column of graphs (A, C, E, G, and I) shows dose–response curves for α-MSH in the presence of 10−6 M (squares, red lines), 10−7 M (tri- angles, blue lines), 10−8 M (inverted triangles, green lines), or absence (diamonds, black lines) of AgRP(83–127) peptide at the zebrafish melanocortin receptors indicated. The right column of graphs (B, D, F, H, and J) shows dose– response curves for α-MSH in the presence of the same doses of AgRP2(93–136) peptide. α-MSH–stimulated activity of zebrafish melanocortin receptors was monitored using a cAMP-dependent β-galactosidase assay. Data points indicate the averages of triplicate determinations. Experiments were performed in triplicate, and graphs were drawn and analyzed using Graphpad Prism. Used with permission.

At t = 24hr, the reaction comes to equilibrium. The major product is identified as the fully oxidized protein by a loss of 10amu. The folding reaction was then quenched by addition of glacial acetic acid, purified by C4 RP-HPLC and lyophilized. The purified, folded protein was quantified by amino acid analysis, revealing that 1.6mg +/- 0.4mg zAgRP2 was obtained after folding.

Melanocortin Receptor Pharmacology

Pharmacological characterization of the synthetic zAgRP2 was performed at five zebrafish melanocortin receptors: MC1, MC3, MC4, MC5a and MC5b. HEK293 cells stably expressing recombinant forms of the zebrafish receptors were incubated with varying concentrations of the peptide. Levels of cAMP were then monitored after titration with increasing amounts of the competitive ligand α-MSH. As demonstrated in Figure 3, zAgRP is able to antagonize α-MSH at MC1r, MC3r and MC4r; however, zAgRP2 is only a competitive ligand at MC1r.

In Vivo Expression of agrp2 mRNA

To further understand the *in vivo* function of zAgRP2, the Cone Lab studied mRNA expression levels in zebrafish embryos. Figure 4 (A-C) shows *agrp2* in situ hybridization images of zebrafish embryos. The dark blue stain signifies high levels of *agrp2* mRNA expression, specifically in the pineal gland of the brain. Quantitative PCR (qPCR) studies of other tissues reveal

agrp2 mRNA levels are most highly expressed in the brain, with lower levels also detected in the testis and dorsal skin (Figure 4D). Furthermore, *agrp2* mRNA was not affected by fasting, as is the case for *agrp* (Figure 4E and F).

In normal adaptive embryos, proMCH and proMCH-like genes (*pmch* and *pmchl*) are affected by exposure to light and dark environments and in turn affect pigmentation (Figure 5A-J). By contrast, embryos treated with Mopholino oligonucleotides (MOs) to knockdown *agrp2* displayed a significantly darker phenotype throughout the body (Figure 5K-Q). In situ hybridization and qPCR studies were also performed on *floating head* (*flh*) mutant embryos. This mutation causes blocked pineal neurogenesis (*15*). Embryos with the *flh* mutation exhibited normal mRNA expression levels of *pomca* and *agrp*, but much lower mRNA expression levels for *pmch*, *pmchl* and *agrp2*. This results in a significantly darker phenotype from wild type (Figure 6A-M).

Implications

Chemical synthesis has long been a means of quickly obtaining sufficient quantities of small peptides for experimental purposes. Full-length agouti and agouti-related peptides are typically range from 125-136 residues in length, and are thereby outside of the threshold for chemical synthesis. However, the C-terminal domain of these peptides is clearly defined, contains all of the necessary receptor binding contacts, and is well within reasonable

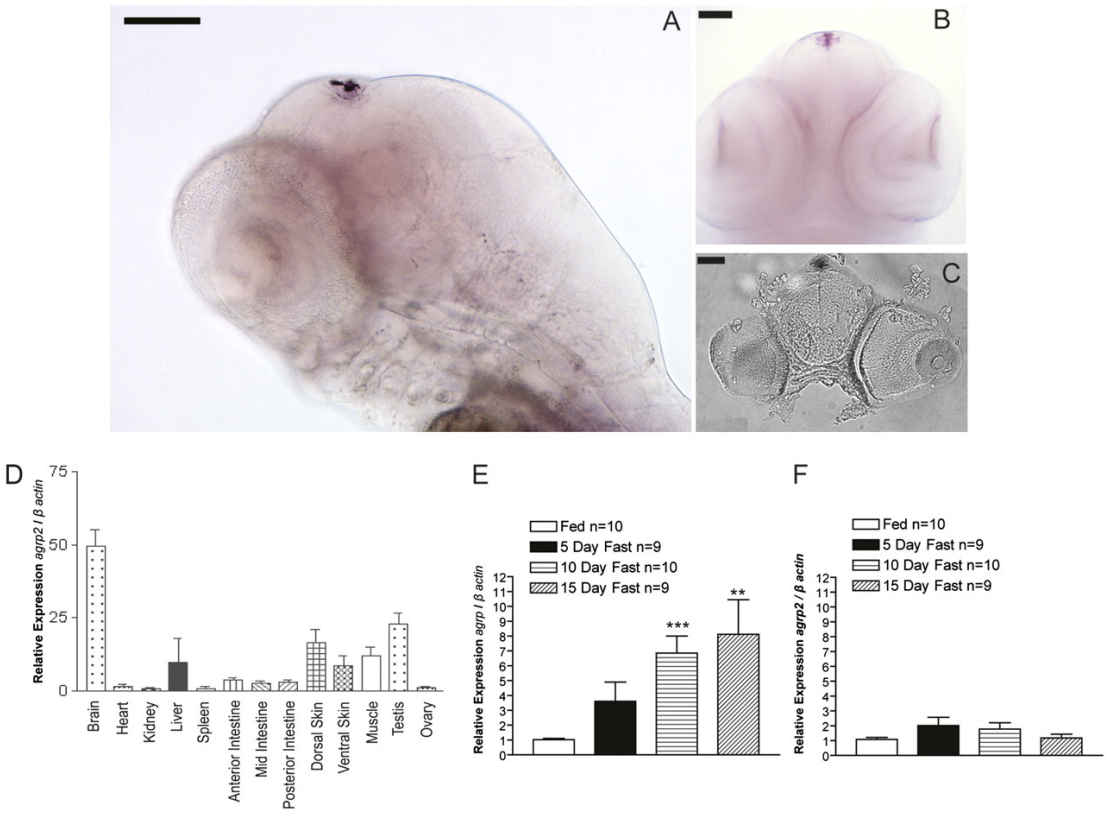

Figure 4. agrp2 is expressed in the zebrafish pineal gland and is not regulated by metabolic state. (A) Lateral view of a 96-hpf whole-mount embryo. Whole-mount in situ hybridization was performed with dig-agrp2 antisense probe followed by Nitro blue tetrazolium chloride/ 5-Bromo-4-chloro-3-indolyl phosphate (NBT/BCIP) color development. (B) Dorsal view of a 72-hpf embryo. (C) Frontal view of a 20-μm section from a 96-hpf embryo hybridized as described in A, then embedded in optimal cutting temperature compound and processed using a cryostat. (D) qPCR analysis of agrp2 with tissues from four adult zebrafish (two male and two female). agrp2 mRNA expression was normalized to β-actin mRNA. (E and F) Relative expression levels of agrp and agrp2 by metabolic state as analyzed by qPCR. One-year-old male fish were fed or fasted for indicated times, and the relative mRNA expression levels of agrp and agrp2 normalized to β-actin were determined from whole-brain tissues. Results are expressed as mean ± SEM, and statistical analyses were done by unpaired t test. **P < 0.01; ***P < 0.001. (Scale bars in A–C: 100 μm). Used with permission

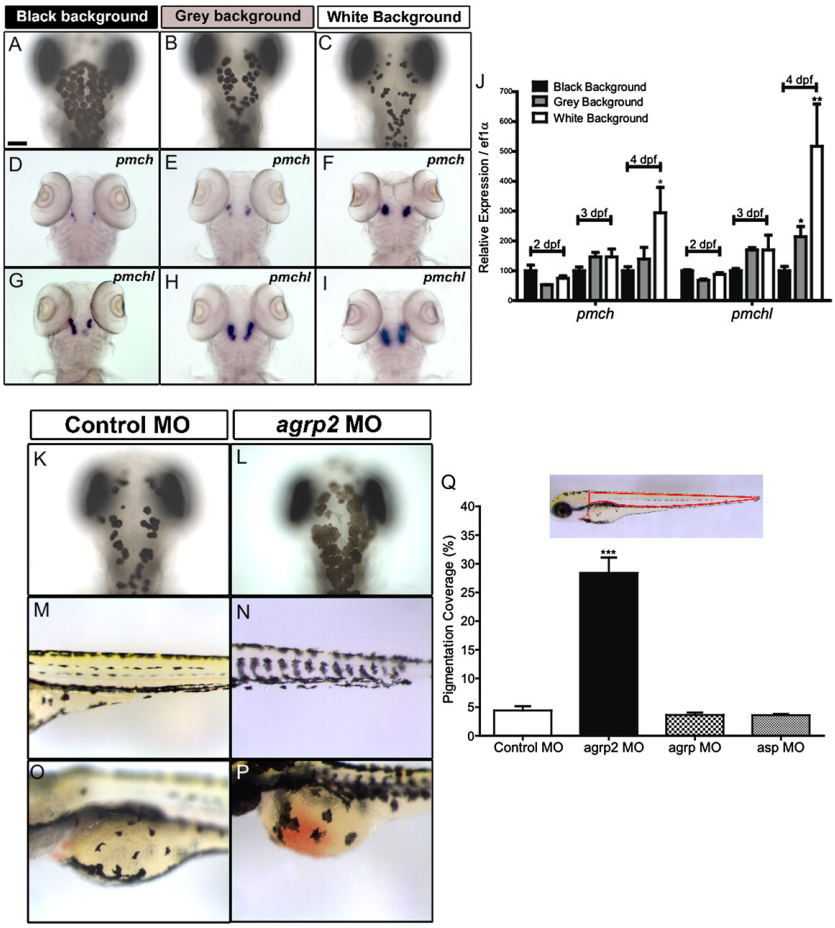

Figure 5. agrp2 is required for melanosome contraction in zebrafish. Control or morpholino-injected embryos were kept in black-, gray-, or white-bottomed Petri dishes with 14-h/10-h light/dark cycle at 28 °C upon fertilization. (A–C) Dorsal melanocytes of (A) black, (B) gray, or (C) white background-adapted wild- type embryos at 4 dpf. (D–I) Whole-mount in situ hybridization of (D–F) *pmch* and (G–I) *pmchl* in black (D and G), gray (E and H), or white (F and I) background-adapted wild-type embryos at 4 dpf. At least 30 embryos for each condition were analyzed. Scale bar: 100 μM. (J) Relative expression levels of *pmch* and *pmchl* were analyzed by real-time qPCR. At 2, 3, and 4 dpf, 30 black, gray, or white background-adapted wild-type embryos were divided into three groups and killed for RNA extraction and cDNA synthesis. mRNA expression was normalized to ef1α mRNA. Results are expressed as mean ± SEM, and statistical analysis was done by unpaired t test. *P < 0.05; **P < 0.01. (K–P) MOs designed to inhibit expression of each of the zebrafish agouti proteins were injected into wild-type zebrafish embryos. Dermal melanocytes were examined at 3–5 dpf at 1200 hours. Photographs show the (K and L) dorsal head, (M and N) lateral trunk, and (O and P) yolk melanocytes in inverted control (K, M, and O) or agrp2 (L, N, and P) antisense MO-injected embryos at 4 dpf at 1200 hours. (Q) Melanosome coverage of the lateral trunk was quantified at 4 dpf using Image J (National Institutes of Health) on agrp2 ATG MO-injected (28.4%, n = 10), agrp ATG MO-injected (3.6%, n = 10), and asp ATG MO-injected (3.5%, n = 10) embryos compared with inverted control MO-injected embryos (4.4%, n = 10). Error bar indicates ± SEM. Statistical significance tested by unpaired t test. ***P < 0.001. Used with permission.

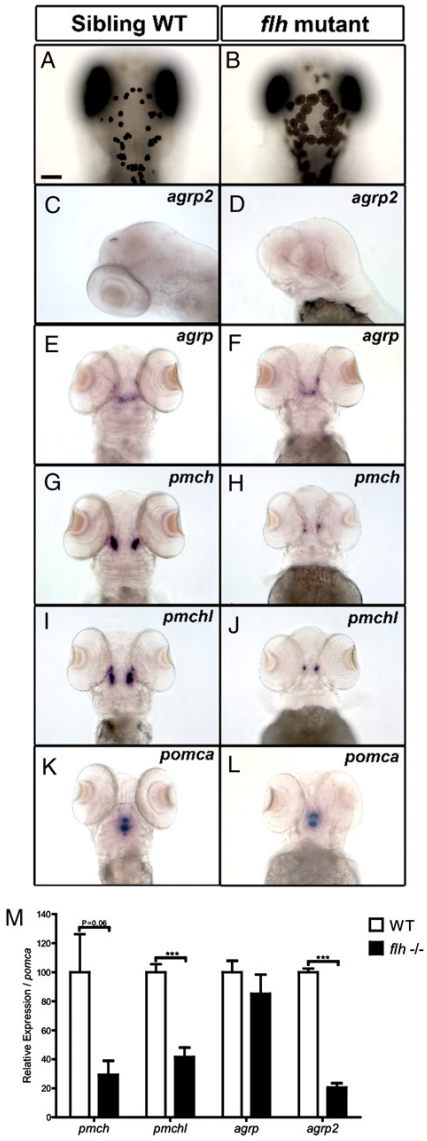

Figure 6. *pmch*, *pmchl*, and *agrp2* are decreased in floating head (*flh*) mutants. *flh*+/− fish were crossed, and 400 zygotes were collected at 0 dpf, with 25% expected to be *flh*−/−. Embryos were kept in egg water, changed daily, with 14-h/ 10-h light/dark cycle at 28 °C. Phenotypically wild-type or *flh*−/− embryos were fixed for whole-mount in situ hybridization (4 dpf) or killed for qPCR analysis (3 dpf). (A and B) Dorsal melanocytes of (A) white background-adapted sibling wild- type or (B) flh−/− embryos at 4 dpf. (C–L) Whole-mount in situ hybridization of (C and D) *agrp2*, (E and F) *agrp*, (G and H) *pmch*, (I and J) *pmchl*, and (K and L) *pomca* in white background-adapted sibling wild-type (C, E, G, I, and K) or *flh*−/− embryos (D, F, H, J, and L) at 4 dpf. At least 15 embryos for each condition were analyzed. (M) Relative expression levels of *agrp*, *agrp2*, *pmch*, and *pmchl* were analyzed by qPCR. Thirty *flh*−/− and 30 phenotypically wild-type embryos (*flh*+/− or *flh*+/+) were divided into three groups and killed at 3 dpf for RNA extraction and cDNA synthesis. mRNA expression was normalized to *pomca* mRNA, and each expression level was further normalized to wild-type expression levels. Results are expressed as mean ± SEM, and statistical analysis was done by unpaired t test. ***P < 0.001. Scale bar: 100 μM.

Used with permission.

limits for solid-phase peptide synthesis. This chapter clearly demonstrates the synthesis of a novel, zebrafish specific, agouti-related protein C-terminal domain from a genetic sequence. Furthermore, zAgRP2$_{93\text{-}136}$ displays oxidative folding properties similar to those observed for other agouti-related proteins. Previous work on agouti and agouti-related C-terminal folding has implicated the two 'CXC' sequence motifs as important contributors to *in vitro* folding stability (*16*). The presence of an aromatic amino acid between the two-cysteine residues allows for π-π interactions, stabilizing the β-hairpin structure, and the formation of a disulfide bridge. As such, the presence of two histidine residues facilitates this process in zAgRP2, enabling *in vitro* oxidative folding.

The zebrafish AgRP sequences both exhibit unique receptor pharmacology when compared to human AgRP. The standard zAgRP clearly has efficacy at MC1r, MC3r and MC4r where hAgRP is unable to antagonize α-MSH at MC1r. Conversely, zAgRP2 is only effective at MC1r within physiologically relevant concentrations (nM). This receptor has long been linked to pigmentation and coat color in vertebrates
(*17*, *18*). Given the receptor specificity, it is reasonable to believe the new agouti-like protein contributes to this pathway in teleost fish. To examine the relevance of zAgRP2 in pigmentation, the Cone lab examined mRNA expression levels in various zebrafish tissues. The results above clearly demonstrate that zAgRP2 is primarily expressed in the pineal and are

supported by previous studies (*19*, *20*). Additionally, unlike normal AgRP, zAgRP2 expression levels are not affected by feeding; indicating that this third sequence is not involved in energy balance and homeostasis.

Knockdown experiments further implicate zAgRP2 in background adaptation. Morpholino oligonucleotides (MOs) are antisense nucleic acid analogs that disrupt small regions of RNA basepairing and prevent interactions with other molecules. This effectively prevents transcription of the target mRNA. Addition of specific MOs against AgRP2 resulted in nearly a six-fold increase in pigmentation of zebrafish embryos when raised against a white background. Expression of *pmch* and *pmchl* is also linked to zAgRP2. Use of AgRP2 MOs results in a significant (>50%) reduction of both pigment-reducing gene mRNAs. Similarly, floating head mutants also showed a significant reduction of mRNA levels of all three genes, however *agrp* and *pomca* all remained within normal levels. These studies clearly link zAgRP2 and the pineal to background adaptation in teleost fish. Moreover, the zebrafish hypothalamus shows the higher Mc1R expression levels than any other tissue. This is in direct contrast to humans, in which Mc1R is primarily expressed in the skin. The zebrafish pineal is known to project to the hypothalamus and signaling by AgRP2 to Mc1R neurons in the hypothalamus would facilitate the interaction (*21*).

The current study outlines a novel pathway in background adaptation and pigmentation specific to teleost fish. The zebrafish provides the ideal

environment for the study of the pineal gland and its role in this physiological process, primarily due to its translucent nature. Photoreceptors in the pineal begin a signal cascade, starting with expression of a third, novel endogenous McR antagonist, zAgRP2. Through interactions at Mc1R in the hypothalamus, MCH expression is increased, causing melanosome aggregation in skin cells. This represents a significant discovery in the melanocortin system and in the understanding of vertebrate evolution.

References

1. Bultman, S. J., Michaud, E. J., and Woychik, R. P. (1992) Molecular characterization of the mouse agouti locus., *Cell 71*, 1195–1204.
2. Chai, B.-X., Neubig, R. R., Millhauser, G. L., Thompson, D. A., Jackson, P. J., Barsh, G. S., Dickinson, C. J., Li, J.-Y., Lai, Y.-M., and Gantz, I. (2003) Inverse agonist activity of agouti and agouti-related protein., *Peptides 24*, 603–609.
3. Berson, D. M., Dunn, F. A., and Takao, M. (2002) Phototransduction by retinal ganglion cells that set the circadian clock, *Science 295*, 1070–1073.
4. Provencio, I., Jiang, G., de Grip, W. J., Hayes, W. P., and Rollag, M. D. (1998) Melanopsin: An opsin in melanophores, brain, and eye, *Proc Natl Acad Sci USA 95*, 340–345.
5. Peirson, S. N., Halford, S., and Foster, R. G. (2009) The evolution of irradiance detection: melanopsin and the non-visual opsins, *Philos Trans R Soc Lond, B, Biol Sci 364*, 2849–2865.
6. BREDER, C. M., and RASQUIN, P. (1950) A preliminary report on the role of the pineal organ in the control of pigment cells and light reactions in recent teleost fishes., *Science 111*, 10–2, illust.
7. Berman, J. R., Skariah, G., Maro, G. S., Mignot, E., and Mourrain, P. (2009) Characterization of two melanin-concentrating hormone genes in zebrafish reveals evolutionary and physiological links with the mammalian MCH system, *J Comp Neurol 517*, 695–710.
8. Kawauchi, H., Kawazoe, I., Tsubokawa, M., Kishida, M., and Baker, B. I. (1983) Characterization of melanin-concentrating hormone in chum salmon pituitaries., *Nature 305*, 321–323.
9. LEE, T. H., and LERNER, A. B. (1956) Isolation of melanocyte-stimulating hormone from hog pituitary gland, *J Biol Chem 221*, 943–959.
10. Gantz, I., and Fong, T. M. (2003) The melanocortin system, *Am J Physiol Endocrinol Metab 284*, E468–74.
11. Kurokawa, T., Murashita, K., and Uji, S. (2006) Characterization and tissue distribution of multiple agouti-family genes in pufferfish, Takifugu rubripes, *Peptides 27*, 3165–3175.
12. Jackson, P. J., McNulty, J. C., Yang, Y.-K., Thompson, D. A., Chai, B., Gantz, I., Barsh, G. S., and Millhauser, G. L. (2002) Design, pharmacology, and NMR structure of a minimized cystine knot with agouti-related protein activity, *Biochemistry 41*, 7565–7572.
13. McNulty, J. C., Thompson, D. A., Bolin, K. A., Wilken, J., Barsh, G. S., and Millhauser, G. L. (2001) High-resolution NMR structure of the chemically-synthesized melanocortin receptor binding domain AGRP(87-132) of the agouti-related protein, *Biochemistry 40*, 15520–15527.

14. Chen, W., Shields, T. S., Stork, P. J., and Cone, R. D. (1995) A colorimetric assay for measuring activation of Gs- and Gq-coupled signaling pathways., *Anal. Biochem. 226*, 349–354.
15. Masai, I., Heisenberg, C. P., Barth, K. A., Macdonald, R., Adamek, S., and Wilson, S. W. (1997) floating head and masterblind regulate neuronal patterning in the roof of the forebrain., *Neuron 18*, 43–57.
16. McNulty, J. C., Jackson, P. J., Thompson, D. A., Chai, B., Gantz, I., Barsh, G. S., Dawson, P. E., and Millhauser, G. L. (2005) Structures of the agouti signaling protein, *J Mol Biol 346*, 1059–1070.
17. Ollmann, M. M., Lamoreux, M. L., Wilson, B. D., and Barsh, G. S. (1998) Interaction of Agouti protein with the melanocortin 1 receptor in vitro and in vivo., *Genes Dev. 12*, 316–330.
18. Lu, D., Willard, D., Patel, I. R., Kadwell, S., Overton, L., Kost, T., Luther, M., Chen, W., Woychik, R. P., Wilkison, W. O., and Cone, R. D. (1994) Agouti protein is an antagonist of the melanocyte-stimulating-hormone receptor, Nature Publishing Group *371*, 799–802.
19. Toyama, R., Chen, X., Jhawar, N., Aamar, E., Epstein, J., Reany, N., Alon, S., Gothilf, Y., Klein, D. C., and Dawid, I. B. (2009) Transcriptome analysis of the zebrafish pineal gland, *Dev Dyn 238*, 1813–1826.
20. Forlano, P. M., and Cone, R. D. (2007) Conserved neurochemical pathways involved in hypothalamic control of energy homeostasis, *J Comp Neurol 505*, 235–248.
21. Yáñez, J., Busch, J., Anadón, R., and Meissl, H. (2009) Pineal projections in the zebrafish (Danio rerio): overlap with retinal and cerebellar projections, *Neuroscience 164*, 1712–1720.

CHAPTER 3

(β-MSH and Obesity)

Structural analysis of a POMC variant responsible for early-onset obesity by NMR Chemical Shift Indexing

(Much of the text and figures of this chapter appeared originally as "A POMC variant implicates β−melanocyte-stimulating hormone in the control of human energy balance." Published in Cell Metabolism 2006 February;3(2):135-140. This work was done in collaboration with the I. Sadaf Farooqi laboratory at the Cambridge Institute for Medical Research, United Kingdom, and is reprinted with permission.)

Abstract

The proopiomelanocortin (POMC) is a prohormone that is produced in various tissues throughout the body and processed by prohormone convertase enzymes to release melanocortin receptor (McR) agonist peptides. In the hypothalamus, prohormone convertase 2 (PC2) produces two high-affinity Mc4R ligands a- and b-melanocyte stimulating hormone (MSH). A-MSH has long been implicated in the regulation of energy balance and homeostasis through McR signaling, however b-MSH has largely overlooked due to the absence of the required PC2 cleavage site to produce this molecule. Here, we examine the structural significance of a genetic POMC variant in the region coding for b-MSH, found in the UK population and implicated in early-onset obesity. Analysis of the chemical shift index (CSI) generated by 2-dimensional NMR of the wild-type and mutant sequences reveals a structural divergence for the mutant peptide away from a turn conformation. We also characterize the receptor binding pharmacology for these agonist sequences, revealing a clear loss of activity. These results suggest a clear physiological role for the b-MSH protein and demonstrate a structural significance for the conserved Tyr residue four positions prior to the receptor recognition sequence.

Introduction

Proopiomelanocortin (POMC) is a pro-hormone found in all vertebrate species that undergoes proteolytic processing to release a multitude of ligands all of which play integral roles in a diverse array of physiological processes throughout the body (*1*). Expression of POMC is highly tissue specific, primarily being produced in the hypothalamus, caudal medulla and anterior pituitary in the CNS as well as in the lymphoid system and skin melanocytes. POMC is originally released as a 241 residue pro-hormone with a 26 amino acid signaling sequence. Further processing of POMC is regulated through tissue specific expression of pro-hormone convertases (PC) (*2*). These enzymes cleave POMC at highly conserved dibasic sites and PC expression specificity regulates the type of ligands released from the pro-hormone.

Tissue expression of prohormone convertase 1 (PC1) in pituitary corticotroph cells and skin melanocytes allows for processing of POMC at three different sites (*3*). This results in the release of N-terminal peptide (NT), Joining peptide (JP), Adrenocorticotropic hormone (ACTH) and b-lipotropin (β-LPH). Both ACTH and β-LPH stimulate adrenal steroidogenesis in the pituitary. Additionally, ACTH is the primary active ligand released in skin melanocytes by PC1 cleavage where it stimulates an increase in cAMP through an interaction with the G protein-coupled melanocortin receptor 1 (Mc1R).

In the hypothalamus, further processing of ACTH, β-LPH, and NT by prohormone convertase 2 (PC2) releases α, β, and γ melanocyte stimulating hormones (MSH), respectively (Figure 1A) (*4*). In a manner similar to ACTH at Mc1R; α, β, and γ-MSH all stimulate cAMP production through interactions at Mc3R and 4r (*5*). All of the MSH peptides released contain the consensus sequence His-Phe-Arg-Trp. This domain serves as the binding and activity domain necessary for interaction at the central Melanocortin receptors, Mc3R and Mc4R. Because of this, all PC2 cleavage products show affinity for both receptors with varying strengths. α and β-MSH both display high affinity binding at both Mc3R and 4R, however γ-MSH exhibits a 50-fold greater binding affinity at Mc3R than at Mc4R (*6*).

The hypothalamic melanocortin system is the subject of many studies due to its link with energy balance and homeostasis, particularly the link between Mc4R activity and feeding behavior. Humans and mice lacking a functional Mc4R exhibit a phenotype of extreme hyperphagia, early onset obesity and hyperinsulinaemia (*7-9*). Similarly, mice containing homozygous mutations preventing the expression or cleavage of POMC are severely obese while heterozygous POMC null mice and humans are predisposed to obesity (*10-12*). Mice lacking an active Mc3R do not display dramatic phenotype changes however they do exhibit abnormalities in body composition later in life (*13*, *14*).

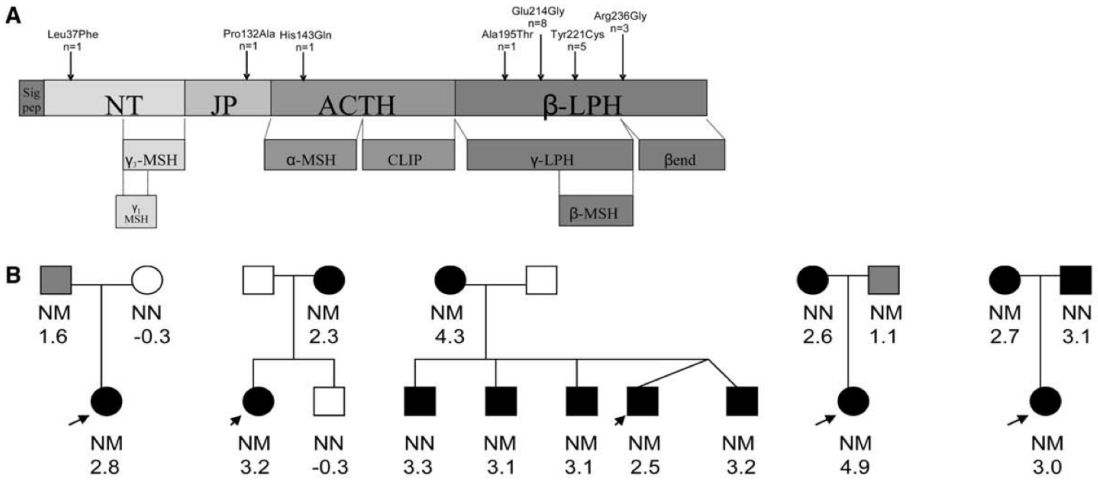

Figure 1. Identification and characterization of Tyr221Cys β-MSH mutation A) Structure of POMC and location of rare missense mutations. B) Cosegregation of Tyr221Cys β-MSH mutation with obesity (black symbols) and overweight (gray symbols) in families. Genotype (N = wild-type allele, M = mutant allele) and BMI sds is denoted. In adults, overweight defined as BMI 25–30 kg/m2, obesity as BMI > 30 kg/m2. In children, overweight defined as >91st and obesity as >99th per- centile for age-adjusted BMI. Arrows indicate the proband of each family. Used with permission.

Table 1. Identification of variants in *POMC*

POMC variants	Obese children (n = 538)	Controls (n = 300)
Nonsynonymous SNPs & insertion		
Leu37Phe	1	0
9 bp insertion (c.297-298insAGCAGCGGC)	51 (9.48%)	28 (9.33%)
Pro132Ala	1	0
His143Gln	1	1 (0.33%)
Ala195Thr	1	0
Glu214Gly	8 (1.49%)	2 (0.67%)
Tyr221Cys	5 (0.93%)	1 (0.33%)
Arg236Gly	3 (0.56%)	2 (0.67%)
Synonymous SNPs		
Cys6Cys	5	0
Ser94Ser	4	0
Ala195Ala	4 (0.74%)	1 (0.33%)
Leu116Leu	8 (1.49%)	7 (2.33%)

Synonymous and nonsynonymous variants in severely obese children and controls.

Recently, the Farooqi research group at the Cambridge Institute for Medical Research, conducted a genetic study of 538 Caucasian children in the UK with severe early onset obesity (with no apparent glucocorticoid issues), to examine POMC alleles for possible mutations. In total, seven different and nonsynonymous (amino acid altering), single nucleotide polymorphisms (SNPs) and one insertion (9bp) mutation were found within the coding region of POMC (Table 1). Of particular interest was a mutation within the coding region for β-MSH, converting Tyr221 to cysteine. This mutant β-MSH was present in five separate probands (nearly 1% of the population studied) and in 1 of 300 control subjects (Figure 1B). Further genetic analysis of the individuals' nearest relatives revealed all of the carriers of this SNP were overweight (BMI 25-30 kg/m^2), with 6 of the 8 family members being obese (BMI > 30 kg/m^2).

The majority of the literature focuses on α-MSH as the primary ligand at Mc4R (*15*, *16*). This is primarily because rodents are the most common experimental species, and the rodent POMC gene lacks the required dibasic PC2 cleavage site necessary to release β-MSH from β-lipotropin (*17*). However, this overlooks in vivo studies that indicate β-MSH is equally potent in appetite suppression (*6*). In light of these findings, it is possible that β-MSH plays a vital role in the regulation of energy balance and homeostatis in humans that has yet to be characterized.

To investigate the significance of β-MSH in hypothalamic melanocortin signaling we performed structural and pharmacological studies on both wild type (WT) and mutant (Tyr221Cys) β-MSH. Specifically, my role in this project was to synthesize variants of β-MSH, purify them, and examine the effects on global structure this mutation has through 2-dimensional nuclear magnetic resonance (2D-NMR) NMR spectroscopy. Together, these studies demonstrate a significant role for this melanocortin ligand and identify a structural significance to the Tyr mutant.

Methods

Peptide Synthesis

All peptides were synthesized using Fmoc synthesis on an Applied Biosystems (Foster City, CA) 433A Peptide Synthesizer on a 0.25mmol scale. Syntheses were monitored using the SynthAssist version 2.0 software package. All peptides were assembled on a Rink-amide-MBHA. Amino acids and resins were purchased through NovaBiochem. HBTU was obtained from Advanced Chemtech (Louisville, KY), and all other reagents were purchased from Sigma-Aldrich (St. Louis, MO). Fmoc deprotection was achieved using a 1% hexamethyleneimine (HMI) and 1% 1,8-Diazabicyclo[4.5.0]-undec-7-ene (DBU) solution in DMF. Deprotection was monitored by conductivity and continued until the conductivity level returned to the baseline, then synthesis continued. Deprotection times ranged from 2.5-7 minutes. Couplings used 4 equivalents Fmoc-amino acid in HBTU/DIEA for all amino acids except pre-activated Fmoc-Cys(trt)-OPfp. A 3-fold excess of Fmoc-Cys(trt)-OPfp was dissolved in 1.5mL 0.5M HOAt/DMF with no DIEA for coupling. All peptides were N-terminal acetylated by reacting with 0.5M acetic anhydride in DMF for 5 minutes. Fully synthesized peptide resins were split into 3 reaction vessels, washed with DCM and dried. A solution of 12mL TFA containing 200mL each of TIS/EDT/liquefied Phenol (as scavengers) was added to each reaction vessel of dry peptide resin and incubated for 1.5h. The resin was filtered and washed with 1mL TFA and the combined filtrate and wash was then added to

90mL cold dry diethyl ether for precipitation. The precipitate was collected by centrifugation and the ether was discarded. The pellet was dissolved in 40mL 1:1 H_2O:ACN (0.1% TFA) and lyophilized.

Purification and Identification

Peptides were purified by RP-HPLC on Vydac (Hesperia, CA) preparative C18 columns. Fractions were collected and analyzed by ESI-MS on a Micromass (Wythenshawe, UK) ZMD mass spectrometer to confirm the correct molecular weight. In each case the major peak was found to be the peptide, and fractions, which contained the peptide as a major constituent, were combined and lyophilized.

2D-NMR Studies

Two-dimensional ^{1}H NMR (2D-NOESY and 2D-TOCSY) performed on peptides corresponding to the b-MSH segment of POMC was used to assign chemical shifts in both wild-type and a mutant with a Tyr221Ser mutation. Ser was used instead of Cys since, at NMR concentrations, free -SH groups tend to form disulfides. Identical experiments were later performed on the Tyr221Cys mutant (unpublished results). For flexible peptides, a negative CSI indicates a turn or helical structure and a positive CSI indicates the presence of extended, β sheet conformers (18, 19).

NMR samples for both wild-type and mutant contained approximately 3.0 – 4.0 mM peptide in 50 mM d4 acetate buffer, and 10% D2O, with the pH adjusted to 4.5 – 4.8. Chemical shifts were referenced to an internal standard (TMSP). Spectra were acquired at approximately 2.0˚C. Parameter settings for the two-dimensional spectra were standard for peptides and small proteins and similar to those used previously.

Competitive Binding and Receptor Activation Studies

All Pharmacolological experiments were conducted by collaborators in the Farooqi lab, at Cambridge Institute for Medical Research.

Competitive binding assays were done using whole HEK293 cells stably expressing wild-type Mc4R exposed to tracer amounts of [125I]NDP-MSH, and the ability of increasing concentrations of β-MSH or [Cys5] β-MSH to inhibit radioligand binding was measured as described previously (8). All wild-type and mutant peptides were obtained from Bachem.

Receptor activation assays were completed using HEK293 cells transiently transfected with wild-type MC4R and cotransfected with a cAMP-dependent luciferase reporter construct. cAMP/Luciferase reporter assays were performed as described previously (8).

Results and Discussion

2D-NMR

The melanocortin agonists ranging in length from 11 amino acids (γ-MSH) to 18 amino acids (β-MSH) and lack ridged secondary structure. Still, small peptides are known to form local structural motifs in absence of a full domain. Tyr221 is highly conserved in POMC, being present in all species from teleost fish to humans. A Tyr residue is also conserved at the same position in α-MSH and γ-MSH in all mammalian species. To determine the significance of this residue in the global structure we examined the two-dimensional NMR spectrum of wild-type β-MSH and two synthetic mutants: Tyr221Ser and Tyr221Cys. Initially, the serine mutant was used to avoid potential disulfide cross-linking during the experiment. Serine is a common substitute for cysteine in these types of experiments due to its similar physical size and helical propensity in protein structure.

Backbone alpha-proton (αH) chemical shifts of the peptides were obtained by two-dimensional ^{1}H-^{1}H nuclear overhauser enhancement spectroscopy (NOESY) and total correlation spectroscopy (TOCSY), and are expressed in Table 2. Comparison of the β-MSH αH chemical shifts to the standard chemical shifts of random-coil amino acids allows for generation of a chemical shift index (CSI) (*18*). This CSI is then used for convenient inspection of the three-dimensional structure. Briefly, secondary structure motifs alter aH chemical shifts. Helical or turn motifs shift peaks upfield, with

respect to random coil, creating a negative CSI value. Likewise, β-strand shift peaks downfield, creating a positive CSI. Inspection of the residues immediately following the mutation shows a clear downfield trend for both β-MSH mutants when compared to wild-type (Figure 2A). Specifically, Arg222 and Met223 showed downfield shifts greater than 0.07ppm. Strikingly, a moderate downfield shift for His225 was also observed. This indicates a loss of helical-propensity following the mutation, including the first residue of the binding domain (HFRW).

Receptor Binding and Activation

Collaborators in the Farooqi Lab studied the effects of this mutation on receptor though competitive binding and cAMP-reporter assays. Binding studies were performed on HEK293 cells stably expressing Mc4R. Cells were then pre-incubated with a radio-ligand (^{125}I NDP-MSH) before titration of the desired peptide. Figure 2B and C shows the displacement of the radio-ligand by wild-type b-MSH and the Tyr221Cys mutant. The mutant peptide exhibits a near 10-fold reduction in binding affinity compared to wild-type (WT β-MSH IC_{50} = 67.2 +/- 43.0nM compared to b-MSH Y221C IC_{50} = 797.1 +/- 261nM). Similarly, a luciferase reporter assay for cAMP production demonstrated that the mutant peptide induces less maximal cAMP with a nearly 20-fold larger half-maximal concentration (Y221C EC_{50} = 1.95nM compared to EC_{50} = 0.1nM for WT).

Table 2. α-Proton chemical shifts of synthetic β-MSH constructs

	Wild-type		Tyr221Ser		Tyr221Cys	
	αH	stdev	αH	stdev	αH	Stdev
R222	4.215	.0005	4.325	.001	4.317	.001
M223	4.365	.001	4.447	.0005	4.465	.001
E224	4.158	.001	4.162	.001	4.171	.001
H225	4.529	.001	4.568	.001	4.578	.0005
F226	4.495	.0005	4.493	.001	4.500	.001
R227	4.204	.001	4.201	.001	4.208	.001
W228	4.638	.002	4.635	.001	4.641	.001

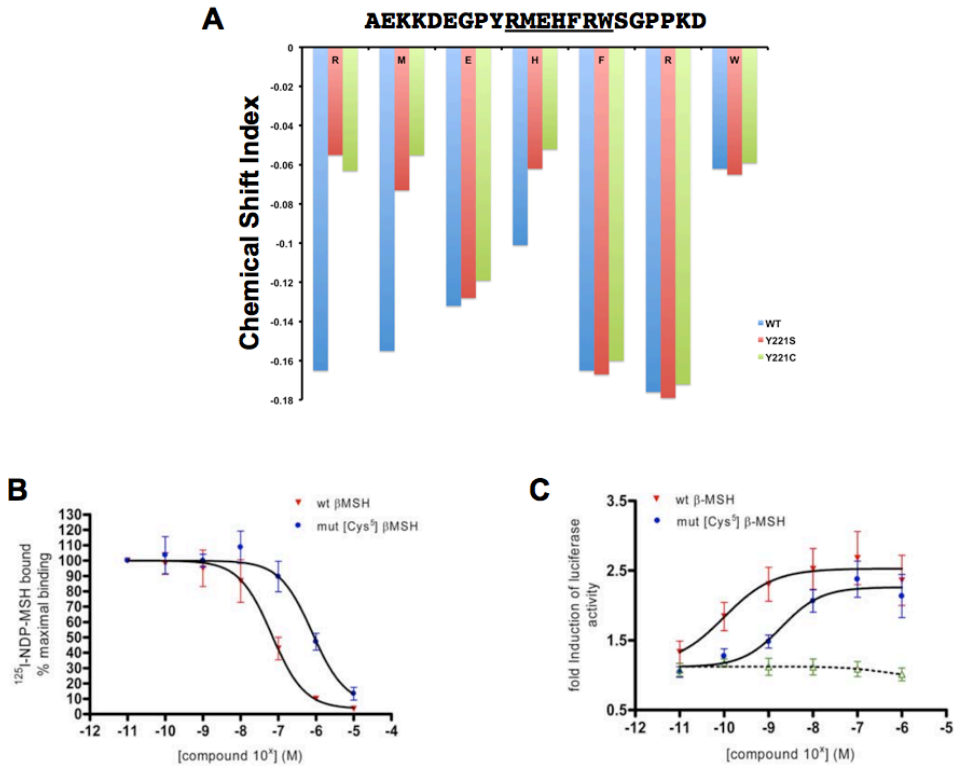

Figure 2. (a) Comparison of the Chemical Shift Index (CSI = experimental chemical shift—consensus random coil chemical shift) values between wild-type and mutant β-MSH. Throughout the segment Arg-Met-Glu-His-Phe-Arg-Trp, the CSIs for all peptides were indicating the presence of turns (values ranging from 20.01 to 20.24). For the Arg-His residues following the mutation the wild-type sequence showed a significantly greater tendency to form turns relative to the mutants. (b) [Cys5] b-MSH binds to MC4R with lower affinity than b-MSH. Whole HEK293 cells stably expressing wild-type MC4R were exposed to tracer amounts of [125I]NDP-MSH, and the ability of increasing concentrations of b-MSH or [Cys5] b-MSH to inhibit radio-ligand binding was measured as described previously. Data are expressed as a per- centage of maximum counts of [125I]NDP-MSH binding to MC4R. Each point represents the mean (6SEM) of four independent experiments in triplicate. (c) [Cys5] b-MSH has a markedly reduced ability to stimulate production of cAMP. Graphs indicate responses of wild-type, mutant, and control constructs to a logarithmic increase in b-MSH concentration. cAMP/Luciferase reporter assays were performed as described previously (Yeo et al., 2003). Open symbols denote mock transfected controls. Each point represents the mean (6SEM) of eight independent experiments performed in quadruplicate.

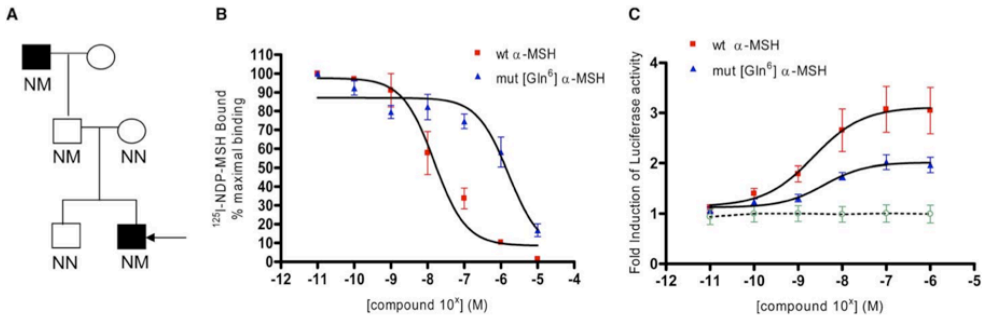

Figure 3. His143Gln α-MSH mutation A) Cosegregation of His143Gln α-MSH mutation with obesity (black symbols). N = wild-type allele, M = Mutant allele. B) [Gln6] α-MSH binds to Mc4R with lower affinity than α-MSH. Data is expressed as a percentage of maximum counts of [125I]NDP-MSH binding to MC4R. Each point represents the mean (6SEM) of four independent experiments in triplicate. C) [Gln6] α-MSH has a markedly reduced ability to stimulate production of cAMP. Open symbols denote mock-transfected controls. Each point represents the mean (6SEM) of eight independent experiments performed in quadruplicate.

Implications

Agonism of the central melanocortin receptors has been a key area of research because of its correlation with genetic obesity. Understanding the factors required for stimulation of these receptors, and thereby reducing the feeding response, can provide valuable information in the design of treatments for various metabolic disorders. The findings above clearly demonstrate a functional role for β-MSH in the Mc4R signaling pathway and identify a single-point genetic mutation, outside of the receptor-binding motif, that strongly correlates with early-onset obesity. Strikingly, the genetic studies conducted by the Farooqi Lab suggest that β-MSH may be more important than a-MSH, the currently accepted standard ligand of Mc4R.

Along with the Tyr221Cys mutation, the genetic study also revealed a single proband with a α-MSH mutation that coincides with the binding domain (His143Gln). As expected, the mutant α-MSH displayed reduced receptor binding and activation (Figure 3). Further genetic investigation revealed the grandfather of the proband was heterozygous for the mutant allele and was obese. Interestingly, the transferring parent exhibited a lean phenotype. This is in direct contrast with the β-MSH allele. Of the five probands heterozygous for the mutant, none of the carrier family members were found to be lean. Six of the eight family were obese and two transferring parents were over-weight (25%). Taken together, this implies that disruption of α-MSH binding may be a contributing factor, but is insufficient to completely explain the obese

phenotype of the proband. The mutant β-MSH allele is both more penetrant and sufficient to explain the obese phenotype, suggesting a greater role for β-MSH in the hypothalamus than α-MSH.

Pharmacological studies of the mutant β-MSH show a full 10-fold reduction in receptor binding affinity and even greater reduction in receptor activation (compared to wild-type), suggesting a disruption to the structure of the ligand. NMR analysis of the WT peptide indicates a clear helical or turn propensity immediately following Tyr221 and through the HFRW domain. Mutation of this residue to either Cys or Ser (both helix breaking) alters this region, shifting towards random coil. Moreover, the cysteine mutant appears to have a more potent effect on this motif, causing a greater shift in all but one αH peaks following the mutation. It is possible that a turn motif is responsible for presenting the HFRW sequence to the receptor-binding pocket and that a tyrosine is necessary to form this turn. All POMC derived McR agonists conserve a tyrosine residue at the same position (four amino acids prior to the putative binding region), further supporting this hypothesis (*2*).

In total, the studies presented herein describe a previously unknown significance for β-MSH in central melanocortin signaling. This peptide is a potent agonist of Mc4R in the hypothalamus and is possibly a more relevant ligand than α-MSH. The genetic studies identify a novel mutation in the POMC gene, in the region coding for β-MSH, strongly correlating to early-onset obesity. NMR analysis of the mutant peptide elucidates a structural role

for Tyr221 in the local structure of the ligand. This is the first evidence of a mutation outside of the HFRW region that contributes to MSH structure and may provide important insight to pharmaceutical researchers attempting to design high-affinity ligands for melanocortin receptors.

References

1. Hadley, M. E., and Haskell-Luevano, C. (1999) The proopiomelanocortin system, *Ann N Y Acad Sci 885*, 1–21.
2. Bertagna, X. (1994) Proopiomelanocortin-derived peptides., *Endocrinol. Metab. Clin. North Am. 23*, 467–485.
3. Seidah, N. G., and Chrétien, M. (1999) Proprotein and prohormone convertases: a family of subtilases generating diverse bioactive polypeptides, *Brain Res 848*, 45–62.
4. Pritchard, L. E., Turnbull, A. V., and White, A. (2002) Pro-opiomelanocortin processing in the hypothalamus: impact on melanocortin signalling and obesity., *J Endocrinol 172*, 411–421.
5. Gantz, I., and Fong, T. M. (2003) The melanocortin system, *Am J Physiol Endocrinol Metab 284*, E468–74.
6. Abbott, C. R., Rossi, M., Kim, M., AlAhmed, S. H., Taylor, G. M., Ghatei, M. A., Smith, D. M., and Bloom, S. R. (2000) Investigation of the melanocyte stimulating hormones on food intake. Lack Of evidence to support a role for the melanocortin-3-receptor., *Brain Res 869*, 203–210.
7. Farooqi, I. S., Keogh, J. M., Yeo, G. S. H., Lank, E. J., Cheetham, T., and O'Rahilly, S. (2003) Clinical spectrum of obesity and mutations in the melanocortin 4 receptor gene, *N Engl J Med 348*, 1085–1095.
8. Yeo, G. S. H., Lank, E. J., Farooqi, I. S., Keogh, J., Challis, B. G., and O'Rahilly, S. (2003) Mutations in the human melanocortin-4 receptor gene associated with severe familial obesity disrupts receptor function through multiple molecular mechanisms, *Hum Mol Genet 12*, 561–574.
9. Huszar, D., Lynch, C. A., Fairchild-Huntress, V., Dunmore, J. H., Fang, Q., Berkemeier, L. R., Gu, W., Kesterson, R. A., Boston, B. A., Cone, R. D., Smith, F. J., Campfield, L. A., Burn, P., and Lee, F. (1997) Targeted disruption of the melanocortin-4 receptor results in obesity in mice, *Cell 88*, 131–141.
10. Cone, R. D. (2005) Anatomy and regulation of the central melanocortin system, *Nat Neurosci 8*, 571–578.
11. Coll, A. P., Farooqi, I. S., Challis, B. G., Yeo, G. S. H., and O'Rahilly, S. (2004) Proopiomelanocortin and energy balance: insights from human and murine genetics, *J Clin Endocrinol Metab 89*, 2557–2562.
12. Challis, B. G., Coll, A. P., Yeo, G. S. H., Pinnock, S. B., Dickson, S. L., Thresher, R. R., Dixon, J., Zahn, D., Rochford, J. J., White, A., Oliver, R. L., Millington, G., Aparicio, S. A., Colledge, W. H., Russ, A. P., Carlton, M. B., and O'Rahilly, S. (2004) Mice lacking pro-opiomelanocortin are sensitive to high-fat feeding but respond normally to the acute anorectic effects of peptide-YY(3-36), *Proc Natl Acad Sci USA 101*, 4695–4700.

13. Chen, A. S., Marsh, D. J., Trumbauer, M. E., Frazier, E. G., Guan, X. M., Yu, H., Rosenblum, C. I., Vongs, A., Feng, Y., Cao, L., Metzger, J. M., Strack, A. M., Camacho, R. E., Mellin, T. N., Nunes, C. N., Min, W., Fisher, J., Gopal-Truter, S., MacIntyre, D. E., Chen, H. Y., and van der Ploeg, L. H. (2000) Inactivation of the mouse melanocortin-3 receptor results in increased fat mass and reduced lean body mass., *Nat Genet 26*, 97–102.
14. Butler, A. A., Kesterson, R. A., Khong, K., Cullen, M. J., Pelleymounter, M. A., Dekoning, J., Baetscher, M., and Cone, R. D. (2000) A unique metabolic syndrome causes obesity in the melanocortin-3 receptor-deficient mouse., *Endocrinology 141*, 3518–3521.
15. Mountjoy, K. G., and Wong, J. (1997) Obesity, diabetes and functions for proopiomelanocortin-derived peptides, *Mol Cell Endocrinol 128*, 171–177.
16. Poggioli, R., Vergoni, A. V., and Bertolini, A. (1986) ACTH-(1-24) and alpha-MSH antagonize feeding behavior stimulated by kappa opiate agonists., *Peptides 7*, 843–848.
17. Challis, B. G., Pritchard, L. E., Creemers, J. W. M., Delplanque, J., Keogh, J. M., Luan, J., Wareham, N. J., Yeo, G. S. H., Bhattacharyya, S., Froguel, P., White, A., Farooqi, I. S., and O'Rahilly, S. (2002) A missense mutation disrupting a dibasic prohormone processing site in pro-opiomelanocortin (POMC) increases susceptibility to early-onset obesity through a novel molecular mechanism, *Hum Mol Genet 11*, 1997–2004.
18. Mielke, S. P., and Krishnan, V. V. (2004) An evaluation of chemical shift index-based secondary structure determination in proteins: influence of random coil chemical shifts, *J Biomol NMR 30*, 143–153.
19. Wishart, D. S., Sykes, B. D., and Richards, F. M. (1992) The chemical shift index: a fast and simple method for the assignment of protein secondary structure through NMR spectroscopy., *Biochemistry 31*, 1647–1651.

CHAPTER 4

(AgRP and Glycosaminoglycans)

Exploring a possible interaction between AgRP constructs and Glycosaminoglycans by Isothermal Titration Calorimetry

Abstract

The Agouti-Related Protein (AgRP) is a paracrine signaling molecule expressed in the hypothalamus that acts an as antagonist at the melanocortin 3 and 4 receptors (Mc3R and 4R). AgRP is originally expressed as a 112 residue protein with an unstructured N-terminal domain followed by a structured C-terminal domain with an inhibitor cystine knot (ICK) core. The N-terminal domain is post-translationally removed to release the fully active C-terminal peptide $AgRP_{83-132}$. This peptide has been further minimized by chemical synthesis to a 34 residue construct with full McR activity in vitro. Here we examine the differential binding strength of three AgRP constructs with the polysaccharide heparin to investigate a possible interaction with cell-surface proteoglycans through isothermal titration calorimetry (ITC). The full C-terminal construct has a near 50-fold stronger dissociation constant (K_d= 21nM) for heparin than does the N-terminal domain (K_d of roughly 1μM). Furthermore, the minimized C-terminal domain, $miniAgRP_{83-120}$ has no affinity for heparin at all. These studies suggest a possible physiological function for the C-terminal loop that has previously not been characterized.

Introduction

The melanocortin system is a family of receptors and ligands that regulate many important physiological processes throughout the body. The five receptors in this system, Mc1R-Mc5R, belong to the super-family of G-protein coupled receptors (GPCRs), and exhibit high tissue expression specificity (*1*, *2*). Possibly the most unique aspect of this system is the presence of two endogenously expressed competitive antagonists, agouti-signaling protein and agouti-related protein (ASIP and AgRP). These proteins have the ability to compete with melanocortin agonists for the same receptor binding site, causing a reduction in cAMP production (*3*).

ASIP and AgRP share many sequential and structural similarities. Both antagonists are excreted as 111 residue proteins with two distinct structural domains (*4*). The N-terminal domain is largely unstructured and contains regions of hydrophobic amino acids as well as regions of acidic amino acids. By contrast, the C-terminal domain is highly structured and contains several basic residues (*5*, *6*). Ten sequentially and spatially conserved cysteine residues fully oxidize to form five disulfide bonds, producing three distinct loops and provide the rigid structure to the C-terminal domain. Interestingly, three of the disulfide bridges create an inhibitor cystine-knot (ICK) fold that s predominantly found in marine cone snail toxin and scorpion venom (*7*).

The C-terminal domains of ASIP and AgRP have a greater than 40% sequence identity and contain all of the necessary motifs for high-affinity

receptor binding *in vitro* (*8*). Despite this homology, these peptides exhibit distinct melanocortin receptor selectivity. AgRP is primarily expressed in the arcuate nucleus of the hypothalamus where it interacts with Mc3R and Mc4R and participates in energy balance and homeostasis (*3*). AgRP is the most potent orexigenic compound and has long been studied for its role in genetic obesity (*9*-*12*). Mutations causing overexpression of AgRP lead to severe hyperphagia, obesity and diabetes-like symptoms. ASIP, on the other hand, is normally expressed in the skin where it interacts with Mc1R and affects coat color and skin pigmentation (*13*). Upon binding to the receptor, reduction in cAMP signals for production of pheomelanin, producing a yellow coat color in mammals.

Despite the wealth of knowledge regarding the function of the C-terminal domain, little is known about the physiological role of the unstructured N-terminal region of AgRP. Previous work demonstrates that the N-terminal domain of ASIP is required for full activity at Mc1R *in vivo*. He et al. postulate that this domain interacts with the membrane-bound glycoprotein attractin (Atrn) (*14*). Mice expressing an attractin truncate exhibit a strong agonist phenotype (dark coat color). The C-terminal domain exhibits no binding affinity for attractin by surface plasmon resonance, however the N-terminal domain was found to have a dissociation constant of 0.7μM. This is roughly 100-fold weaker than the binding strength ASIP has for Mc1R. Researchers hypothesize that attractin acts as a low-affinity accessory

receptor of ASIP. Upon binding to attractin, ASIP may then form a ternary complex with Mc1R, although no evidence of this complex has been detected. Initial studies by Reizes et al. suggested a similar interaction for AgRP exists in the hypothalamus, facilitated by syndecans (*15*). They show that transgenic mice expressing a syndecan variant that is maintained on the surface of cell membranes in the CNS, are significantly more obese than their wild-type littermates. Using nitrocellulose blotting techniques, they also show that this syndecan variant, a heparan sulfate proteoglycan (HSPG), exhibits affinity for full-length ASIP and AgRP, but not C-terminal AgRP. However, this is in conflict with recent reports demonstrating the N-terminal domain of AgRP acts as a pro-domain, and is post-translationally cleaved away *in vivo* (*16-18*).

The focus of this chapter is to further study the interaction of glycosaminoglycans (GAGs) with the N- and C-terminal domains of AgRP. The mounting evidence for the C-terminal construct $AgRP_{83-132}$ as the fully-active *in vivo* ligand does not preclude syndecans from participating in the AgRP signaling pathway. One of the primary roadblocks to studying the N-terminal domain is that at 60aa in length it is too large for chemical synthesis. Similarly, previous attempts to express this protein through recombinant techniques have produced little success, most probably due to immediate processing of the protein in the cytosol. Furthermore, *in vitro* cleavage of full-length AgRP by commercially available proteases that recognize the native cleavage site is both expensive and inefficient (*17*). The first goal of this

chapter is to demonstrate the creation of a variant AgRP sequence with a non-native tobacco etch virus (TEV) protease recognition sequence for the reliable production of N-terminal AgRP. Next, isothermal titration calorimetry (ITC) is used to obtain important binding thermodynamic data that blotting techniques are unable to resolve. The data presented here clearly demonstrate a possible interaction for heparan sulfate proteoglycans (HSPGs) and C-terminal $AgRP_{83-132}$ and is stronger than any interaction between HSPGs and the N-terminal domain. The results also suggest a potential physiological significance for a non-ICK region of AgRP that has previously not been characterized.

Methods

Site-Directed Mutagenesis

The GeneTailor™ Site-Directed Mutagenesis system (Invitrogen) was used to add A TEV-protease recognition site to full-length AgRP DNA maintained within the Pet16B vector (previously characterized by Jackson et al.). Synthetic oligonucleotides were designed according to specifications of the kit, with the forward primer containing 18-nucleotide overlap to the 5' side of the mutation and 12-nucleotide overlap to the 3' side.

Forward Primer:

5'CAGGACCGCGAGCCCCGCGAAAACCTGTACTTCCAGTCCTCACGTCGC

Reverse Primer:

5'GCGGGGCTCGCGGTCCTGCAGGTCTAGTAC

Methylated plasmid was amplified with the mutagenic primers using 2.5 units of Platinum Taq DNA polymerase High Fidelity. Standard PCR cycle temperature and durations were used, with elongation step duration of 6min. The resulting PCR product was purified by 1% agarose gel electrophoresis and isolated by GFX Spin column (GE Healthcare). Verification of mutagenesis was achieved by DNA sequencing at UC Berkeley.

Expression of Full-Length AgRP

E.coli BL21-Star competent cells were transformed with the mutant Pet16B plasmid and grown in LB Miller broth containing 100mg/mL ampicillin

at 37^{o}C until OD_{600}=0.6, then induced with 1mM IPTG for 4 hours. Induced cells were centrifuged at 4000rpm at 4^{o}C for 30min. Cell pellets were resuspended in 8M Urea, 0.1M Tris, pH = 8.0 and lysed via hyperbaric cell disruption. Cell lysate was centrifuged at 9000rpm at 4^{o}C for 60min to remove cellular debris, and the supernatant was loaded onto nickel-chelated sepharose (GE Healthcare) and washed with lysis buffer until A_{280} returned to baseline. Resin was then washed with 6M GuHCl, 0.1M Tris, 25mM imidazole, pH=8.0 until A_{280} again returned to baseline. Full-length AgRP mutant was then eluted from the resin with 6M GuHCl, 0.1M Tris, 500mM imidazole, pH=8.0. The eluent was reduced with 100mM DTT and incubated at 37^{o}C to remove non-native disulfide bridges. Fully-reduced recombinant protein was purified by C4 RP-HPLC (Vydac) with water/acetonitrile (0.1% TFA) and lyophilized.

Peptide Synthesis & Purification

AgRP (83-120, C105A) was synthesized using Fmoc synthesis on an Applied Biosystems 433A Peptide Synthesizer on a 0.25-mmol scale and monitored using the SynthAssist 2.0 software package. All peptides were assembled on a Rink-amide-4-methyl- benzhydrylamine resin, and preactivated Fmoc-Cys(trt)-OPfp was used. All amino acids and resins were purchased through Nova-Biochem. HBTU 2-(1H-benzotriazole-1-yl)-1,1,3,3-tetramethylurnium hexafluorophosphate (HBTU) was obtained from Advanced

Chemtech, and all other reagents were purchased from Sigma- Aldrich. Fmoc deprotection was achieved using a 1% hexame- thyleneimine (HMI) and 1% 1,8-diazabicyclo[4.5.0]-undec-7-ene (DBU) solution in dimethyl formamide (DMF). Deprotection was monitored by conductivity and continued until the conductivity level returned to the baseline, then synthesis continued. Deprotection time ranged from 2.5 to 7 min. Coupling used four equivalents Fmoc- amino acid in HBTU/N,N-Diisopropylethylamine (DIEA) for all amino acids except the preactivated cysteine. A threefold excess of Fmoc-Cys(trt)-OPfp was dissolved in 1.5 mL 0.5 M 1-Hydroxy-7- azabenzotriazole/DMF with no DIEA for coupling. The peptides were N-terminal acetylated by reacting with 0.5 M acetic anhydride in DMF for 5 min. Fully synthesized peptide resin was split into three reaction vessels, washed with dichloromethane, and dried. A solution of 8 mL TFA containing 200 µL each of triisopropylsilane/1,2-ethanedithiol/liquefied Phenol (as scavengers) was added to each reaction vessel of dry peptide resin for 1.5 h. The resin was filtered and washed with 1 mL TFA, and the combined filtrate and wash was then added to 90 mL cold dry diethyl ether for precipitation. The precipitate was collected by centrifugation, and the ether was discarded. The pellet was dissolved in 40 mL 1:1 H2O:CAN (0.1% TFA) and lyophilized. Peptide purification was achieved by RP-HPLC on Vydac C18 preparative columns. Fractions were collected and analyzed by ESI-MS on a Micromass ZMD mass spectrometer to confirm the correct molecular weight. In each case the major peak was

found to be the peptide, and fractions, which contained the peptide as a major constituent, were combined and lyophilized.

Oxidative Folding

Air oxidative folding of both AgRP constructs was accomplished by dissolving the unfolded peptide into folding buffer (2.0 M GuHCl/0.1 M Tris, 3 mM reduced glutathione, 400 μM oxidized glutathione, pH 8) at a peptide concentration of 0.1 mg/mL) and stirring for 24 h. Folding was monitored for both peptides by RP-HPLC (C18 analytical column for miniAgRP and C4 analytical column for FL-AgRP), which revealed a single peak in each case, with the folded material shifted to an earlier retention time than the fully reduced peptide. The folded products were again purified by RP-HPLC as above, and identity confirmed as the fully oxidized products by ESI-MS (miniAgRP 83-120: 4381amu, FL-AgRP-TEV mutant: 15402amu).

Processing of Full-length AgRP by TEV-Protease and CNBr

C-terminal $AgRP_{83-132}$ was produced by proteolytic cleavage of the oxidized full-length mutant. Proteolysis was achieved by incubation of lyophilized full-length protein (0.1mg/mL) in 50mM NaAc, pH=5.5 with 10:1 protein:TEV ratio, at room temperature with slight agitation for 24hr. Protein fragments were purified by C4 RP-HPLC as described above and identified by ESI-MS. The resulting N-terminal expression fragment was further

processed by CNBr to remove the His-purification tag. A solution of 0.1mg/ML protein with 20x CNBr in 0.1M HCl was incubated in the absence of light for 24hr at room temperature. The solution was then diluted with 6M GuHCl, 0.1% TFA and purified by C4 RP-HPLC, with two distinct peaks corresponding to cleaved and uncleaved protein. N-terminal $AgRP_{26\text{-}82\text{-}ENLYFQ}$ was identified by ESI-MS. Cleavage was calculated to be roughly 50% effective by HPLC peak integration. Purified N- and C-terminal fragments were lyophilized for later use.

Isothermal Titration Calorimetry

ITC buffer (pH=8) was prepared with 50mM HEPES, 5mM $MgCl_2*6H_2O$ and 1mM $CaCl_2$ (Sigma). ITC buffer was used to make 50μM peptide solutions and 1mM heparin (Sigma, H-3393). Resulting solutions were placed in 2kDa cutoff Slide-A-Lyzer cartridges (Thermo) and dialyzed together in 2L ITC buffer for 24hr. After dialysis all solutions were degased for 2min. 2mL of the target peptide was then added to the sample cell and 2mL of Di H_2O was added to the reference cell. The heparin solution was placed into the injection syringe. ITC experiments were performed on a Microcal VP-ITC machine and monitored using the Origin 7.0 software package with the thermostat set to 25°C. Heparin was titrated in at 2μL increments with constant stirring and the temperature allowed to equilibrate between injections.

Results & Discussion

Expression of a Full-Length AgRP Variant

The in vivo cleavage product $AgRP_{83-132}$ is well within the limits of solid-phase peptide synthesis and has been commercially available for some time. However, the N-terminal domain of AgRP is very difficult to chemically synthesize due to several factors, including length (62 residues), extended hydrophobic regions and numerous beta-branched amino acids. This sequence is similarly difficult to express in bacterial cell lines. To obtain sufficient quantities of N-terminal AgRP, a construct was designed based on the full-length AgRP sequence.

Previous work by Pilgrim Jackson utilized a vector containing the sequence for MKΔ5-$AgRP_{25-132}$ with a 9xHis-tag (for purification), to express full-length AgRP for NMR studies (*16*). Normally, proprotein convertases proteolytically cleave AgRP following Arg82, however duplicating this reaction *in vitro* is both inefficient and expensive. The tobacco etch virus (TEV) protease is a highly efficient protease that is very specific for the recognition sequence ENLYFQ-X, where X is either a Gly or Ser (*19*). This protease cleaves between the Gln and X residues and has been shown to have no star-activity. Moreover, expression systems for this protease have been developed, making it economical to work with and optimize expression systems around (*20*). Using the site-directed mutagenesis protocol from Invitrogen, I added a TEV protease recognition site of ENLYFQ between

Arg82 and Ser83. This new construct would be able to release the natural C-terminal product found in vivo, with an N-terminal peptide that also contained the six-residue TEV recognition site.

The design of the mutagenic primers requires an overlapping region of 15-20 nucleotides in length on the 5' side of the mutation, and another 10 nucleotides on the 3' side of the mutation. The size of the mutation must also be less than 21 bases. Utilizing the native Ser83 allows for an addition of only 6 amino acids, or 18 bases total, which is well within the upper limit. Figure 1 shows the primer design and the resulting DNA sequencing after mutagenesis, demonstrating the incorporation of the TEV sequence. E.coli cells were then transformed with the new plasmid and standard IPTG expression procedures were used to induce AgRP synthesis. Following induction, cells were pelleted and stored at -20 ^{o}C for later use.

Purification and Folding of Full-Length AgRP

To isolate the bacterial expression product, cell pellets were resuspended in lysis buffer containing 8M Urea buffered to pH = 8.0 and added to a hyperbaric cell disruptor for lysis. The resulting solution was then centrifuged to remove cellular debris, and the supernatant added to a nickel chelating column for purification. Figure 2a shows the resulting FPLC chromatogram, which exhibits three low-resolution peaks: the loading peak, the wash peak, and the elution peak. HPLC of the elution peak confirmed the

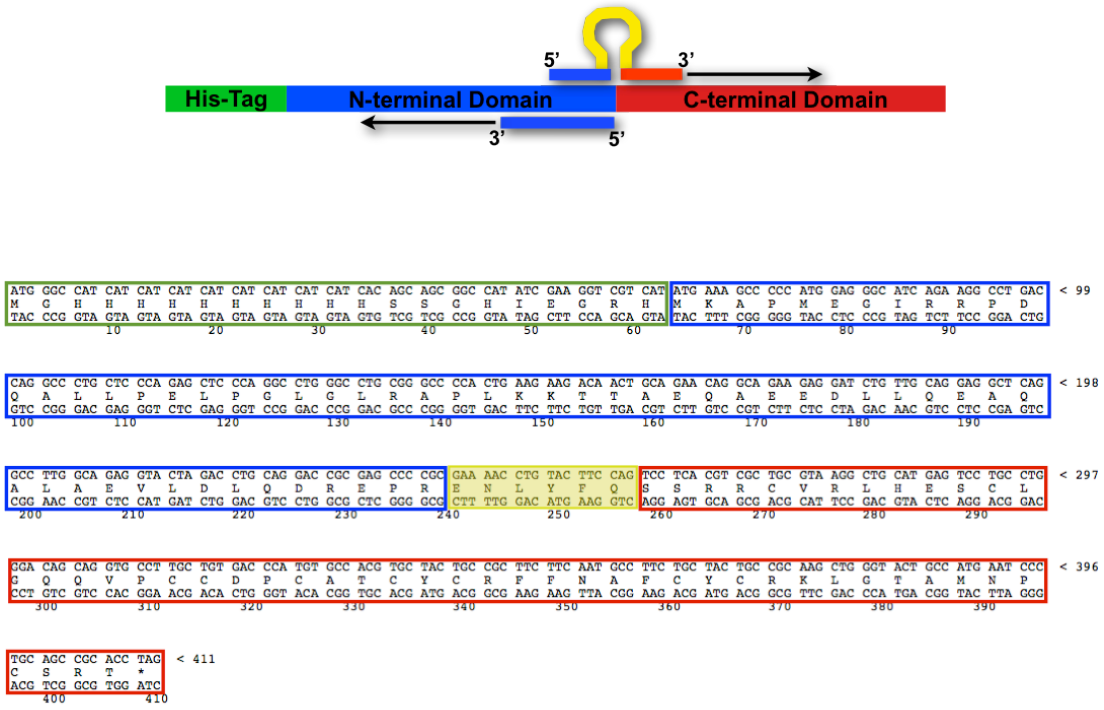

Figure 1. (above) Diagram of primer design adding a TEV-protease recognition site (yellow). The forward primer contained overlapping regions in the N-terminal (blue) and C-terminal (red) domains, while the reverse primer only identified the N-terminal domain. Sequencing results are shown, highlighting all regions of the protein expression sequence (below).

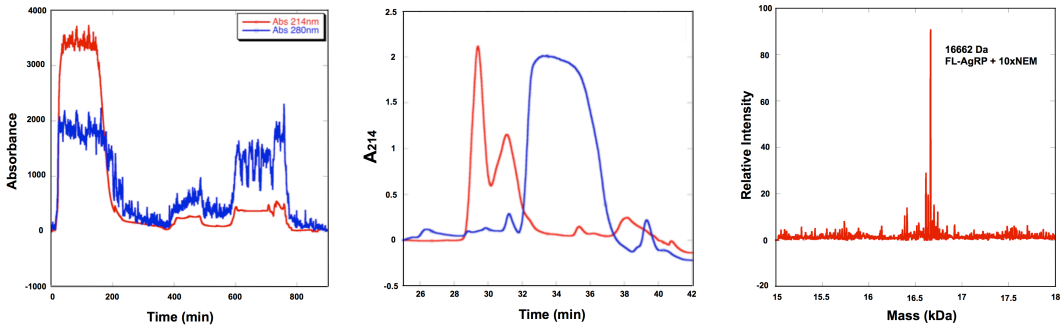

Figure 2. Expression and purification of recombinant full-length AgRP with a TEV protease recognition site. (A) FPLC chromatogram showing loading, wash, and elution peaks from a nickel-chelating column. (B) RP-HPLC purification of FL-AgRP. Expression multiple expression products were resolved with the expected mass (red), resulting from improper disulfide connectivity. Reduction by DTT (blue) results in a single peak with the expected mass of 15410 Da. (C) ESI-MS of reduced FL-AgRP modified by NEM, demonstrating 10 free thiols in the protein.

presence of two products within the mass range for partially folded full-length AgRP. Subsequent reaction with DTT yielded a single broad peak, with the mass of fully-reduced AgRP construct (Fig 2b). Further confirmation of AgRP expression was achieved by reacting the reduced peptide with N-ethylmaleimide (NEM). This chemical modifies free thiols, adding a mass of roughly 125 amu per modification. Reaction with NEM for 24hr produced a protein with a mass corresponding to 10 NEM modifications (Fig 2c).

To form the proper disulfide connectivity, full-length AgRP was allowed to air-oxidize in mild denaturing conditions, at pH = 8.0 in the presence of the red-ox coupling agents oxidized and reduced glutathione. The reaction was gently agitated for 24hr and then quenched by lowering the pH. The resulting HPLC chromatogram displays a single peak at a lower retention time and mass 10amu lower than observed for the unfolded protein (Figure 3a).

Cleavage of Full-Length AgRP

The purified and folded full-length AgRP construct was then ready to be processed to release the two domains for binding studies. Multiple trials were conducted to determine the optimum cleavage conditions for the TEV protease. Figure 3b shows efficient processing of AgRP under mildly acidic conditions (pH = 5.5), producing three very distinct peaks corresponding to folded $AgRP_{83\text{-}132}$, N-terminal AgRP, and TEV protease, respectively. The C-terminal fragment was lyophilized and saved for ITC.

The His-tag was removed from the N-terminal fragment by cyanogen bromide, utilizing the native methionine residue of MKΔ5-AgRP. Using a 30-fold molar excess CNBr, cleavage of the N-terminal fragment was roughly 50% efficient after incubation for 24hr, producing the native peptide $AgRP_{26\text{-}82\text{-}ENLYFQ}$ (Figure3c). Although this was not the desired yield, it did provide enough material for ITC experiments (roughly 2mg).

Binding of Melanocortin Ligands to Heparin

Cell surface proteoglycans are characterized by their long glycosaminoglycan chains. Two of the most common GAGs found are heparin and heparan sulfate (21). These two GAGs are composed of similar disaccharide units, with heparin being more highly sulfated. Heparin is readily available as a heterogeneous mixture of varying length and is commonly used in ITC procedures.

Three AgRP constructs were tested by ITC for possible interactions with heparin: $AgRP_{26\text{-}82\text{-}ENLYFQ}$, $AgRP_{83\text{-}132}$, and $miniAgRP_{83\text{-}120}$. A 1.0mM solution of heparin was made, assuming a molecular weight of 9000amu. This solution was then titrated into a well containing 50μM solution containing one of the ligands. The Micro Calorimeter VP-ITC measures the amount of heat released upon addition of titrant and gives an output of energy needed to return the reaction vessel to the baseline temperature. Results indicate that $AgRP_{83\text{-}132}$ binds heparin with 21 ±13nM affinity, with the N-terminal fragment

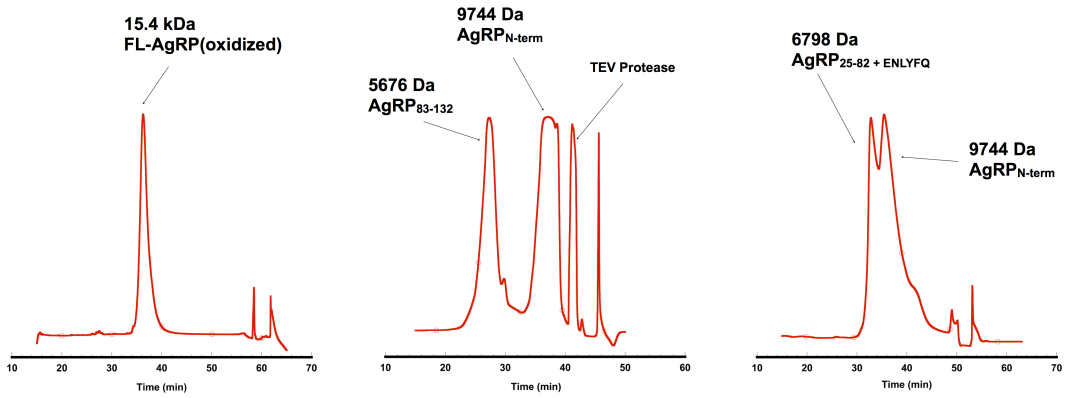

Figure 3. Folding and processing of recombinant AgRP. (A) RP-HPLC of folded FL-AgRP. (B) RP-HPLC of TEV-protease digestion of FL-AgRP. Three peaks resolved correspond to C-terminal AgRP, N-terminal domain with affinity purification tag, and TEV-protease, respectively. (C) CNBr removal of affinity tag from the N-terminal fragment. Roughly 50% cleavage was observed.

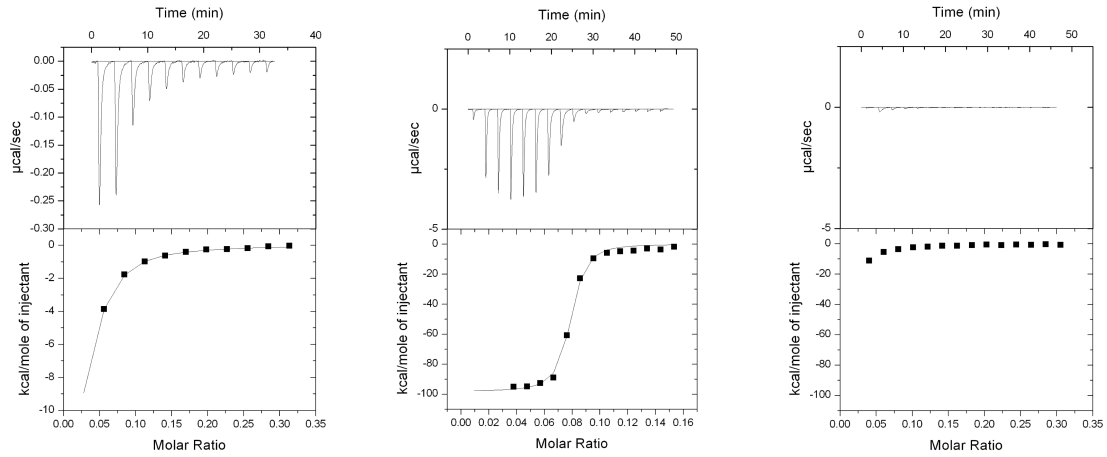

Figure 4. Isothermal Titration Calorimetry of AgRP sequences. N-terminal AgRP (left) displayed a K_d = 0.98 ± 11μM for heparin, with $AgRP_{83-132}$ (center) binding much more strongly, K_d = 27.7 ± 13nM. The synthetic minimized peptide, $miniAgRP_{83-120}$ (right), showed no affinity for heparin.

exhibiting a dissociation constant of roughly 1 μM (Figure 4a and b). By contrast, the minimized C-terminal construct miniAgRP$_{83-120}$ shows no affinity for heparin (Figure 4c).

Implications

The results presented above clearly demonstrate a high affinity interaction between the C-terminal domain of AgRP$_{83-132}$ and the glycosaminoglycan heparin that is nearly 50-fold stronger than observed for the N-terminal domain. Probably the most studied protein-GAG interaction involves the chemokine family of peptides and receptors (*21*, *22*). Like melanocortin antagonists, chemokines are small, disulfide-rich proteins. In many cases, the physiological activity of these proteins is regulated through an equilibrium interaction with cell surface proteoglycans and soluble GAGs. ITC experiments, similar to those implemented here, found that chemokines have a K_d for heparin ranging from 0.39μM to 2.63μM, and that this binding strength is enough to disrupt protein binding to the receptor (*22*). The 1mM dissociation constant observed for N-terminal AgRP would suggest the mechanism proposed for syndecan involvement has some merit, however, given the strength of the interaction with AgRP$_{83-132}$, it is unlikely that the unstructured region would be able to compete.

It is generally accepted that the active *in vivo* form of AgRP is the structured C-terminal domain from Ser83-Thr132. This form has been shown

to have 10-fold greater binding constant and inhibit cAMP production at far lower doses. Studies on synthetic AgRP constructs have identified a minimized version of this domain, miniAgRP$_{87\text{-}120}$, that maintains full receptor binding and activity *in vitro* (*8*, *23*). Despite this, a modified miniAgRP containing the natural four N-terminal residues (83-120), showed no affinity for heparin. If a physiological role for GAG binding to AgRP does exist, this result suggests the final 12 residues that create the “C-terminal loop” play an important part in facilitating this process.

Analysis of the chemokine literature gives credence to this hypothesis. GAGs are highly negative glycopolymers and bind to specific sequential or structural motifs of basic amino acids. IL-8 contains 13 basic residues scattered throughout its primary sequence, creating a very positive electrostatic surface environment. Despite this, the GAG binding domain has been narrowed down to just five amino acids: Lys20, Arg60, Lys64, Lys67, and Arg68 (*22*). Four of these are sequentially close while Lys20 relies on protein folding to bring it within close proximity to provide the patch of basic residues required for binding. Figure 5 contrasts the surface electrostatic environment of AgRP$_{83\text{-}132}$ and miniAgRP$_{83\text{-}120}$. AgRP$_{83\text{-}132}$ only has seven basic residues, but two of them reside in the final loop. Structurally, the final disulfide bond brings Arg131 within close proximity to the ICK core and creates a similar patch of positive surface charge. Removing this final loop

dramatically alters the electrostatics of the minimized protein and is the most likely cause of the disrupted GAG binding in the minimized peptide.

In conclusion, the works presented here describe a potential physiological relevance for C-terminal AgRP binding with glycosaminoglycans that was previously suggested for the N-terminal domain. Based on comparison of the dissociation constants, it is unlikely that the N-terminal domain would be able to out compete the full C-terminal domain for binding. This interaction is believed to be facilitated by a region of basic residues that are brought within close proximity through protein folding and requires the C-terminal loop. This loop is not required for high affinity receptor binding in vitro, and would represent the first discovery of a function for this region of the peptide. Furthermore, the techniques used demonstrate a reliable method for the expression of recombinant a AgRP sequence and subsequent processing by TEV-protease and CNBr to release both domains of the protein. The ITC binding experiments provided binding data that were able to narrow the critical binding motif for GAG binding and provide motivation for further study into the physiological relevance of this interaction.

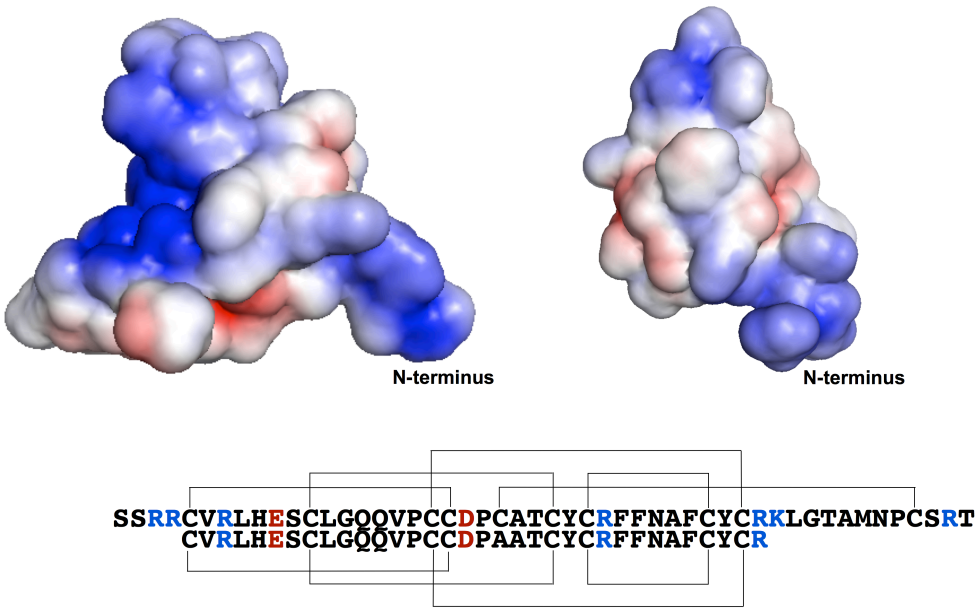

Figure 5. Surface electrostatics of $AgRP_{83-132}$ and $miniAgRP_{83-120}$ as computed by the apbs software package for MacPyMOL. Formation of disulfide bridges brings sequentially distant basic residues within close proximity in vivo. Removal of the C-terminal loop in miniAgRP disrupts a large positively charged area, potentially causing the elimination of GAG binding.

References

1. Tatro, J. B. (1996) Receptor biology of the melanocortins, a family of neuroimmunomodulatory peptides, *Neuroimmunomodulation 3*, 259–284.
2. Gantz, I., and Fong, T. M. (2003) The melanocortin system, *Am J Physiol Endocrinol Metab 284*, E468–74.
3. Ollmann, M. M., Wilson, B. D., Yang, Y. K., Kerns, J. A., Chen, Y., Gantz, I., and Barsh, G. S. (1997) Antagonism of central melanocortin receptors in vitro and in vivo by agouti-related protein., *Science 278*, 135–138.
4. Willard, D. H., Bodnar, W., Harris, C., Kiefer, L., Nichols, J. S., Blanchard, S., Hoffman, C., Moyer, M., Burkhart, W., and Weiel, J. (1995) Agouti structure and function: characterization of a potent alpha-melanocyte stimulating hormone receptor antagonist, *Biochemistry 34*, 12341–12346.
5. McNulty, J. C., Thompson, D. A., Bolin, K. A., Wilken, J., Barsh, G. S., and Millhauser, G. L. (2001) High-resolution NMR structure of the chemically-synthesized melanocortin receptor binding domain AGRP(87-132) of the agouti-related protein, *Biochemistry 40*, 15520–15527.
6. McNulty, J. C., Jackson, P. J., Thompson, D. A., Chai, B., Gantz, I., Barsh, G. S., Dawson, P. E., and Millhauser, G. L. (2005) Structures of the agouti signaling protein, *J Mol Biol 346*, 1059–1070.
7. Yu, B., and Millhauser, G. L. (2007) Chemical disulfide mapping identifies an inhibitor cystine knot in the agouti signaling protein., *FEBS Lett 581*, 5561–5565.
8. Jackson, P. J., McNulty, J. C., Yang, Y.-K., Thompson, D. A., Chai, B., Gantz, I., Barsh, G. S., and Millhauser, G. L. (2002) Design, pharmacology, and NMR structure of a minimized cystine knot with agouti-related protein activity, *Biochemistry 41*, 7565–7572.
9. Madonna, M. E., Schurdak, J., Yang, Y.-K., Benoit, S., and Millhauser, G. L. (2012) Agouti-Related Protein Segments Outside of the Receptor Binding Core Are Required for Enhanced Short- and Long-term Feeding Stimulation., *ACS Chem. Biol. 7*, 395–402.
10. Hagan, M. M., Rushing, P. A., Pritchard, L. M., Schwartz, M. W., Strack, A. M., van der Ploeg, L. H., Woods, S. C., and Seeley, R. J. (2000) Long-term orexigenic effects of AgRP-(83---132) involve mechanisms other than melanocortin receptor blockade., *Am J Physiol Regul Integr Comp Physiol 279*, R47–52.
11. Joppa, M. A., Ling, N., Chen, C., Gogas, K. R., Foster, A. C., and Markison, S. (2005) Central administration of peptide and small molecule MC4 receptor antagonists induce hyperphagia in mice and attenuate cytokine-induced anorexia, *Peptides 26*, 2294–2301.

12. Flynn, M. C., Plata-Salamán, C. R., and Ffrench-Mullen, J. M. (1999) Neuropeptide Y-related compounds and feeding., *Physiol Behav 65*, 901–905.
13. Lu, D., Willard, D., Patel, I. R., Kadwell, S., Overton, L., Kost, T., Luther, M., Chen, W., Woychik, R. P., Wilkison, W. O., and Cone, R. D. (1994) Agouti protein is an antagonist of the melanocyte-stimulating-hormone receptor, Nature Publishing Group *371*, 799–802.
14. He, L., Gunn, T. M., Bouley, D. M., Lu, X. Y., Watson, S. J., Schlossman, S. F., Duke-Cohan, J. S., and Barsh, G. S. (2001) A biochemical function for attractin in agouti-induced pigmentation and obesity, *Nat Genet 27*, 40–47.
15. Reizes, O., Lincecum, J., Wang, Z., Goldberger, O., Huang, L., Kaksonen, M., Ahima, R., Hinkes, M. T., Barsh, G. S., Rauvala, H., and Bernfield, M. (2001) Transgenic expression of syndecan-1 uncovers a physiological control of feeding behavior by syndecan-3, *Cell 106*, 105–116.
16. Jackson, P. J., Douglas, N. R., Chai, B., Binkley, J., Sidow, A., Barsh, G. S., and Millhauser, G. L. (2006) Structural and molecular evolutionary analysis of Agouti and Agouti-related proteins., *Chem. Biol. 13*, 1297–1305.
17. Creemers, J. W. M., Pritchard, L. E., Gyte, A., Le Rouzic, P., Meulemans, S., Wardlaw, S. L., Zhu, X., Steiner, D. F., Davies, N., Armstrong, D., Lawrence, C. B., Luckman, S. M., Schmitz, C. A., Davies, R. A., Brennand, J. C., and White, A. (2006) Agouti-related protein is posttranslationally cleaved by proprotein convertase 1 to generate agouti-related protein (AGRP)83-132: interaction between AGRP83-132 and melanocortin receptors cannot be influenced by syndecan-3., *Endocrinology 147*, 1621–1631.
18. Pritchard, L. E., and White, A. (2005) Agouti-related protein: more than a melanocortin-4 receptor antagonist?, *Peptides 26*, 1759–1770.
19. Sun, C., Liang, J., Shi, R., Gao, X., Zhang, R., Hong, F., Yuan, Q., and Wang, S. (2012) Tobacco etch virus protease retains its activity in various buffers and in the presence of diverse additives., *Protein Expr. Purif. 82*, 226–231.
20. Miladi, B., Bouallagui, H., Dridi, C., Marjou, El, A., Boeuf, G., Di Martino, P., Dufour, F., and Elm'selmi, A. (2011) Reprint of: A new tagged-TEV protease: Construction, optimisation of production, purification and test activity., *Protein Expr. Purif.*
21. Handel, T. M., Johnson, Z., Crown, S. E., Lau, E. K., and Proudfoot, A. E. (2005) Regulation of protein function by glycosaminoglycans--as exemplified by chemokines, *Annu Rev Biochem 74*, 385–410.
22. Kuschert, G. S., Coulin, F., Power, C. A., Proudfoot, A. E., Hubbard, R. E., Hoogewerf, A. J., and Wells, T. N. (1999) Glycosaminoglycans interact selectively with chemokines and modulate receptor binding and

cellular responses, *Biochemistry 38*, 12959–12968.
23. Haskell-Luevano, C., Monck, E. K., Wan, Y. P., and Schentrup, A. M. (2000) The agouti-related protein decapeptide (Yc[CRFFNAFC]Y) possesses agonist activity at the murine melanocortin-1 receptor, *Peptides 21*, 683–689.

CHAPTER 5

(Super AgRP)

Agouti-Related Protein Segments Outside of the Receptor Binding Core are Required for Enhanced Short and Long Term Feeding Stimulation

Michael E. Madonna[1], Jennifer Schurdak[2], Ying-kui Yang[3], Stephen Benoit[2] and Glenn L. Millhauser[1]

Reproduced with permission from ACS Chemical Biology 2012, 7(2), 395-402

Abstract

The Agouti-Related Protein (AgRP) plays a central role in energy balance by reducing signaling through the hypothalamic melanocortin receptors (McRs) 3 and 4, in turn stimulating feeding and decreasing energy expenditure. Mature $AgRP_{83-132}$, produced by endoproteolytic processing, contains a central region that folds as an inhibitor cystine knot (ICK) stabilized by a network of disulfide bonds; this domain alone carries the molecular features for high affinity McR binding and inverse agonism. Outside of the ICK domain are two polypeptide segments – an N-terminal extension and a C-terminal loop – both completely conserved but of unknown function. Here we examine the physiological roles of these non-ICK segments by developing a panel of modified AgRPs that were administered to rats through intracerebroventricular (ICV) injection. Analysis of food consumption demonstrates that basic (positively charged) residues are essential for potent short and long term AgRP stimulated feeding. Moreover, we demonstrate an approximate linear relationship between protein charge density and 24hr food intake. Next, we developed artificial $AgRP_{83-132}$ analogs with increased positive charge and found that these species were substantially more potent than wild type. A single dose of one protein, designated AgRP-4K, results in enhanced feeding for well over a week and weight gain that is nearly double that of $AgRP_{83-132}$. These studies suggest new strategies for the development

of potent orexigenic species, and may serve as leads for the development of therapeutics for treating wasting conditions such as cachexia.

Introduction

The agouti-related protein (AgRP) is produced in the hypothalamus and acts to stimulate feeding and decrease energy expenditure (*1, 2*). AgRP is a high affinity inverse agonist of the melanocortin 3 and 4 receptors (Mc3R and Mc4R), members of the G-protein coupled receptor (GPCR) superfamily. Transgenic mice that overexpress AgRP exhibit increased feeding, profound weight gain and metabolic imbalances often associated with diabetes (*3*). In humans, AgRP plasma levels correlate with body mass (*4*), while certain polymorphisms predispose individuals to anorexia nervosa (*5, 6*). Because of its potency in stimulating feeding, leading to weight gain, AgRP and its mimetics are considered prime therapeutic leads in the treatment of cachexia, the wasting condition associated with cancer and AIDS (*7*).

There are a number of designed ligands that stimulate feeding, including SHU9119, THP, MBP10, and NBI-30 (*8*), but none are more potent after a single low dose administration than AgRP. Moreover, AgRP's effects are prolonged. A single intracerebroventricular (ICV) AgRP injection produces enhanced feeding for up to seven days (*9*). And animals receiving a dose of AgRP followed 24 hours later by administration of MTII (a melanocortin agonist), return to elevated feeding levels at 48 hours (24 hours after agonist injection) (*10*).

AgRP is produced as a 132 amino acid pro-protein that undergoes proprotein convertase (PC 1/3) cleavage, following residue 82, to release its

cysteine-rich C-terminal domain (Table 1) (*11, 12*). The ten cysteine residues within $AgRP_{83-132}$ form a network of five disulfide bonds, as shown in Figure 1 (*13*). Structure determination by NMR demonstrates that residues 87-120 adopt an inhibitor cystine knot (ICK) fold, a scaffold previously found exclusively in invertebrate toxins (*13*). AgRP is homologous to the agouti signaling protein (ASIP), which is expressed in the skin and controls pigmentation by suppressing signaling through Mc1R. Both proteins share the ICK core region in their respective C-terminal domains (*14*). In contrast to AgRP, however, the ASIP N-terminal domain is retained and binds to attractin, an interaction that is essential for in vivo function (*15*).

In addition to Mc1R binding, ASIP is also capable of high affinity interactions with Mc3R and Mc4R, as demonstrated by the obese phenotype in the lethal yellow $A^{y/a}$ mouse (*3*). In contrast, AgRP binds exclusively to Mc3R and Mc4R (*2*). We recently reported a study using a panel of ASIP/AgRP chimeras with the goal of identifying the specific features in ASIP required for Mc1R affinity (*16*). We found that the ASIP C-terminal loop, just past the ICK core, was critical for Mc1R recognition. Moreover, grafting this loop onto the AgRP ICK core resulted in a protein with a Mc1R K_d of approximately 30 nM. As shown in Figure 1, these studies now complete the characterization of ASIP's functional domains.

In contrast, the functions of the polypeptide segments outside of AgRP's ICK core are unknown (Figure 1). The four residue segment

preceding the ICK core (Ser-Ser-Arg-Arg) and the 13 residue C-terminal loop are both highly conserved among mammals (Table 1), yet deletion of these segments has absolutely no affect on the Mc3R or Mc4R binding affinities or in vitro activity (*17*). Specifically, a mini protein composed of just the AgRP ICK core, residues 87-120, possesses approximately the same Mc3R and Mc4R affinity as $AgRP_{87-132}$ (*17*) and $AgRP_{83-132}$ (*18*), and exhibits equivalent inverse agonism (*19*). AgRP is a strongly cationic protein, and interestingly, five of the seven positively charge amino acids are located in the regions outside of the ICK core (defined by the first and last Cys residues).

To address the functional significance of the segments outside of the ICK core domain in mature $AgRP_{83-132}$ (Figure 1), we performed ICV experiments on Long-Evans rats using a panel of AgRP variants in which select non-ICK components are deleted. We find a remarkable relationship between long term feeding enhancement and net AgRP positive charge, carried mainly by the non-ICK segments. Next, we developed a series of novel AgRP constructs where charge is selectively varied. ICV experiments with these constructs not only supports the charge-feeding relationship, but also lead to the discovery of an AgRP analog that significantly increases initial and long term feeding relative to the wild type protein. Together, these studies demonstrate a critical physiological role for the non-ICK AgRP segments, and suggest new strategies in the development of reagents for treating cachexia and other conditions associated with negative energy balance.

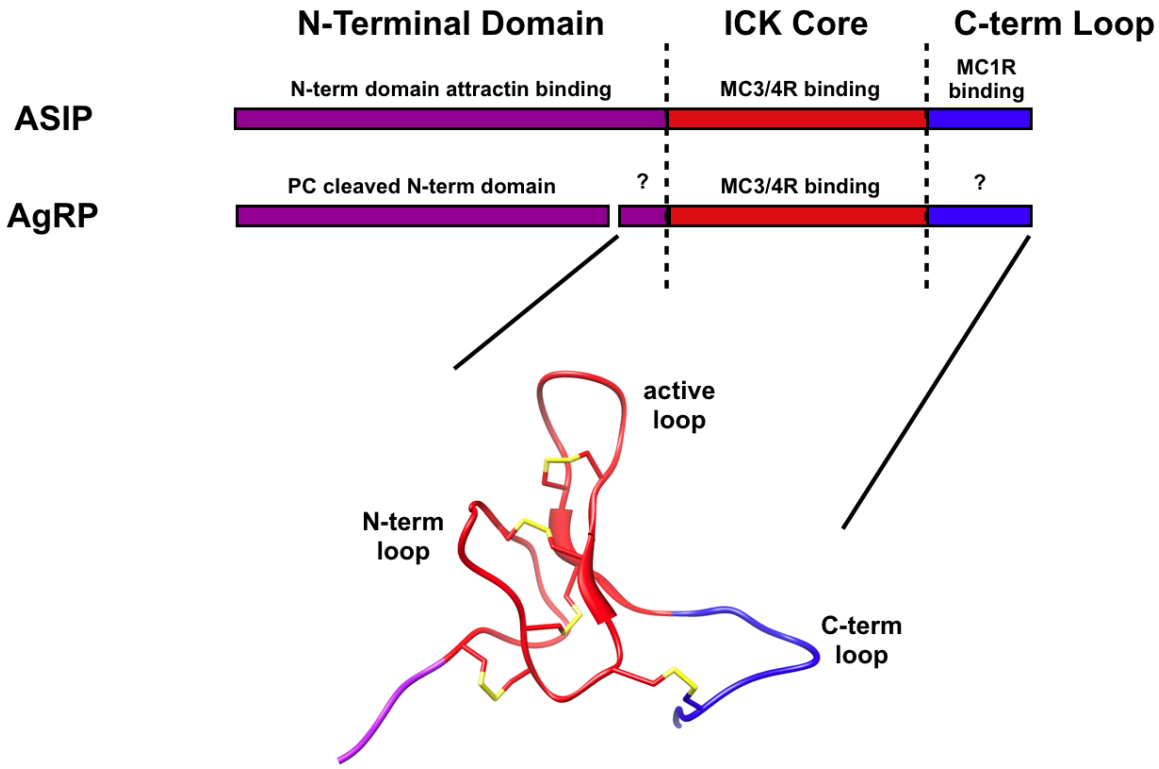

Figure 1. Schematic of ASIP and AgRP structure/function. The sequence diagram (above) illustrates homologous regions of the two proteins and corresponding functional domains. Question marks indicate the two regions of AgRP of conserved but otherwise unknown function. Structure of AgRP(83-132) (below) illustrates the spatial location of the different regions.

Table 1 Agouti Related Protein Sequences

	N-term	Inhibitor Cystine Knot Core	C-Term Loop
Human (83-132)	SSRR	CVRLHESCLGQQVPCCDPCATCYCRFFNAFCYC	RKLGTAMNPCSRT
Cow	SPRR	CVRLHESCLGHQVPCCDPCATCYCRFFNAFCYC	RKLGTTTNPCSRT
Mouse	SPRR	CVRLHESCLGQQVPCCDPCATCYCRFFNAFCYC	RKLGTATNLCSRT
Rat	SPRR	CVRLHESCLGQQVPCCDLCATCYCRFFNTFCYC	RKLGTGTTNLCSRP
Pig	SPRR	CVRLHESCLGHQVPCCDPCATCYCRFFNAFCYC	RKLGTATNPCSRT
Sheep	SPRR	CVRLHESCLGHQVPCCDPCATCYCRFFNAFCYC	RKLGTTT
Designed AgRP Sequences			
AgRP(83-120)	SSRR	CVRLHESCLGQQVPCCDPAATCYCRFFNAFCYC	R
AgRP(87-132)		CVRLHESCLGQQVPCCDPCATCYCRFFNAFCYC	RKLGTAMNPCSRT
AgRP(87-120)		CVRLHESCLGQQVPCCDPAATCYCRFFNAFCYC	R
AgRP-2Q	SSRR	CVRLHESCLGQQVPCCDPCATCYCRFFNAFCYC	RQLGTAMNPCSQT
AgRP-4Q	SSQQ	CVRLHESCLGQQVPCCDPCATCYCRFFNAFCYC	RQLGTAMNPCSQT
AgRP-2K	SSRR	CVRLHESCLGQQVPCCDPCATCYCRFFNAFCYC	RKLKTKMNPCSRT
AgRP-4K	KKRR	CVRLHESCLGQQVPCCDPCATCYCRFFNAFCYC	RKLKTKMNPCSRT

Basic residues in the N-terminal segment and C-terminal loop are shown in blue.

Methods

Peptide Synthesis, Purification and Folding

All peptides were synthesized using Fmoc synthesis on an Applied Biosystems (Foster City, CA) 433A Peptide Synthesizer on a 0.25mmol scale. Syntheses were monitored using the SynthAssist version 2.0 software package. All peptides were assembled on a Rink-amide-MBHA. Amino acids and resins were purchased through NovaBiochem. HBTU was obtained from Advanced Chemtech (Louisville, KY), and all other reagents were purchased from Sigma-Aldrich (St. Louis, MO). Fmoc deprotection was achieved using a 1% hexamethyleneimine (HMI) and 1% 1,8-Diazabicyclo[4.5.0]-undec-7-ene (DBU) solution in DMF. Deprotection was monitored by conductivity and continued until the conductivity level returned to the baseline, then synthesis continued. Deprotection times ranged from 2.5-7 minutes. Couplings used 4 equivalents Fmoc-amino acid in HBTU/DIEA for all amino acids except pre-activated Fmoc-Cys(trt)-OPfp. A 3-fold excess of Fmoc-Cys(trt)-OPfp was dissolved in 1.5mL 0.5M HOAt/DMF with no DIEA for coupling. AgRP(87-132) and AgRP(87-120) were N-terminal acetylated by reacting with 0.5M acetic anhydride in DMF for 5 minutes. Fully synthesized peptide resins were split into 3 reaction vessels, washed with DCM and dried. A solution of 12mL TFA containing 200mL each of TIS/EDT/liquefied Phenol (as scavengers) was added to each reaction vessel of dry peptide resin and incubated for 1.5h. The resin was filtered and washed with 1mL TFA and the combined filtrate

and wash was then added to 90mL cold dry diethyl ether for precipitation. The precipitate was collected by centrifugation and the ether was discarded. The pellet was dissolved in 40mL 1:1 H_2O:ACN (0.1% TFA) and lyophilized.

Peptides were purified by RP-HPLC on Vydac (Hesperia, CA) preparative C18 columns. Fractions were collected and analyzed by ESI-MS on a Micromass (Wythenshawe, UK) ZMD mass spectrometer to confirm the correct molecular weight. In each case the major peak was found to be the peptide, and fractions, which contained the peptide as a major constituent, were combined and lyophilized.

Air oxidative folding of each peptide was accomplished by dissolving the unfolded peptide into folding buffer (2.0M GuHCl/0.1M Tris, 3mM GSH, 400μM GSSG, pH 8) at a peptide concentration of 0.1mg/mL and stirring for 24-36h. Folding was monitored for all peptides by RP-HPLC on a C18 analytical column, which revealed a single peak, in each case, for the folded material that was shifted to an earlier retention time than the fully reduced peptide. The folded product was purified by RP-HPLC on a C18 preparative column and its identity confirmed as the fully oxidized product by ESI-MS. Reinjecting a small sample of the purified peptide on an analytical RP-HPLC column assessed purity of the peptides. Sample purity was determined to be >90%. Quantitative analysis of the peptide concentrations was done by UV absorption.

Rodent Studies

Male Long Evans rats ~10-12 weeks and weighing 250-350g were obtained from Harlan (Indianapolis, IN) and maintained in an AALAC accredited vivarium on a 12 to 12hr light dark cycle. Animals were given ad libitum access to standard rodent chow and water. After a one week habituation period, all animals were deeply anesthetized with a 1-ml/kg dose of (0.22g Ketamine/0.03g Xylazine) and placed into a sterotaxic apparatus with the incisor bars set at +1.0. Subsequently, an indwelling cannula was lowered into the third ventricle using the following coordinates, AP= -2.2, ML=0, DV= -7.0. All animals were allowed to recover for two weeks during which time they regained their pre-surgical body weight. To verify cannula placement, angiotensin II (10ng/µl) was injected into the third ventricle and water consumption was measured over a one hour period. To be included animals had to drink more than 7ml. Animals were injected one hour prior to the beginning of their dark phase using a within subjects paradigm.

Trials were conducted with one control group (receiving saline) and one experimental group (receiving the peptide of interest). After feeding returned to baseline, animals were allowed to re-equilibrate for 1 week before switching the experimental and control groups, and repeating the experiments. Each individual group maintained n > 5. The results of all trials were combined to assess percent baseline, due to differences in time of year and animal subjects. Changes in absolute grams of food intake are not different

than changes in percent baseline. All experiments were run in replicates of 2-3 studies. Errors are expressed as ± SEM.

Pharmacology

The HEK-293 cell line was used for hMc3R and hMc4R transfection. The cells transfected with receptor were cultured in DMEM medium containing 10% bovine fetal serum and HEPES. Cells at 80% confluence were washed twice, and the receptor constructs were transfected into cells using lipofectamine (Life Technologies, Rockville MD). All experiments were run in triplicate and errors are expressed as ± SEM (Table 2).

Binding Assays

Binding experiments were performed using the conditions previously described. Briefly, after removal of the media, cells were incubated with non-radioligand NDP-MSH or AGRP analogues from 10^{-10} to 10^{-6}M in 0.5 ml MEM containing 0.2% BSA and 1 x 10^5 cpm of ^{125}I-NDP-MSH for one hour. The binding reactions were terminated by removing the media and washing the cells twice with MEM containing 0.2% BSA. The cells were then lysed with 0.2 N NaOH, and the radioactivity in the lysate was quantified in an analytical gamma counter (PerkinElmer, Shelton, CT). Nonspecific binding was determined by measuring the amount of ^{125}I-label bound on the cells in the presence of excess 10^{-6} M unlabeled ligand. Specific binding was calculated

by subtracting nonspecifically bound radioactivity from total bound radioactivity.

cAMP Assays

Cellular cAMP generation was measured using a competitive binding assay kit (TRK 432, Amersham, Arlington Heights, IL). Briefly, cell culture media was removed, and cells were incubated with 0.5 ml Earle's Balanced Salt Solution (EBSS), containing the melanocortin agonist NDP-MSH (10^{-10}-10^{-6} M), for one hour at 37˚C in the presence of 10^{-3} M isobutylmethylxanthine. The reaction was stopped by adding ice-cold 100% ethanol (500µl/well). cAMP content was measured as previously described, according to instructions accompanying the assay kit (*33*).

Results and Discussion

Truncated AgRP Variants

ICV injection of AgRP variants was used to assess the physiological role of the protein segments outside of the ICK core, comprising the receptor binding domain (Figure 1). Initial experiments focused on truncated forms of mature $AgRP_{83-132}$ (Table 1). The minimal construct $AgRP_{87-120}$ was designed and investigated in a previous study (*17*). Briefly, this protein lacks both the four residue segment before the ICK domain, and the C-terminal loop. Simple elimination of the C-terminal loop leaves an uncompensated Cys residue at position 105. To avoid the formation of non-native disulfide bonds, residue 105 was mutated to Ala. In addition, Arg120 following the penultimate Cys was retained as it is part of the β-sheet. Our previous NMR work showed that $AgRP_{87-120}$, often referred to as mini-AgRP, folds 100% to a uniform product that retains the ICK structure of the parent protein (*17*). Moreover, dissociation constants measured at Mc3R and Mc4R are equivalent to mature $AgRP_{83-132}$. Two other constructs, $AgRP_{83-120}$ and $AgRP_{87-132}$ were prepared using the same strategies.

ICV injections were administered to Long Evans rats fitted with cannulas in the third ventricle. Proteins were delivered as a single 1.0 nmol dose in 1.0 μL of solution. Feeding and weight were monitored in most cases until consumption returned to baseline values. Results for wild type $AgRP_{83-132}$ and the three truncated variants are shown in Figure 2A.

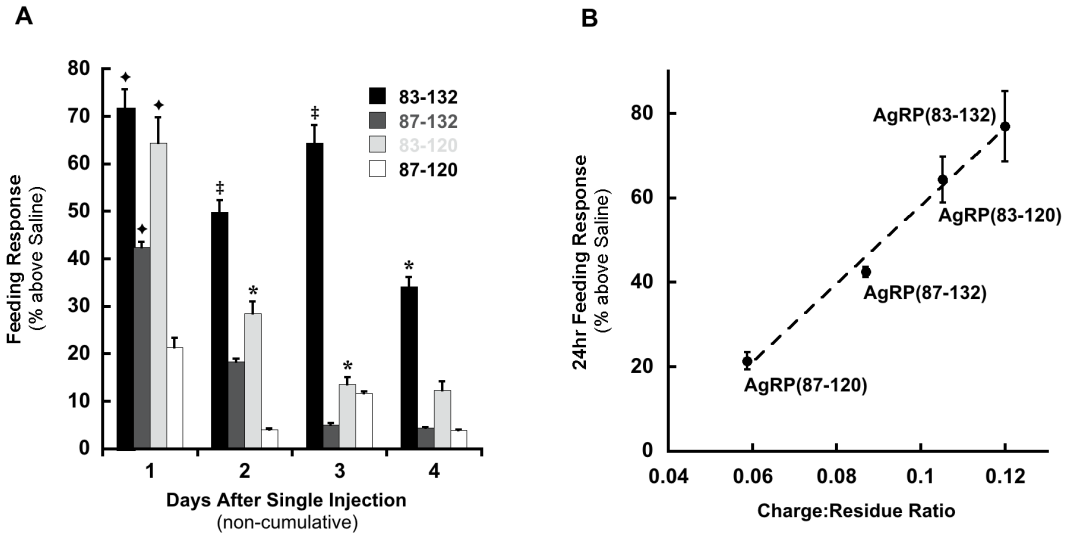

Figure 2. Effect of a single administration of a 1.0 mmol dose of wild type and truncated AgRPs into third cerebral ventricle in male Long-Evans rats. (A) Percent increase over saline at 24 hr, 48 hr, 72 hr and 96 hr after injection (non-cumulative). (B) Net charge density trend of 24hr feeding response above saline control. ✦ $P < 0.001$, ‡ $P < 0.01$, and * $P < 0.05$.

All initially stimulate feeding, as seen in the responses after one day. $AgRP_{83-132}$ is the most potent, stimulating feeding nearly 80% over that of control ($P<0.001$), while mini-AgRP is the least potent. Interestingly, $AgRP_{83-120}$ is essentially equipotent to wild type ($P<0.001$). At three or four days after injection, enhanced feeding relative to control diminishes. Animals dosed with the three truncated variants are almost back to baseline. In contrast, those treated with $AgRP_{83-132}$ are still consuming feed about 30% over control ($P<0.05$ at day 4).

The data in Figure 2A suggest that the four residue non-ICK segment preceding the ICK core is required for rapidly stimulating feeding, whereas both non-ICK segments are needed for long term effects. The significant number of basic, positively charged residues carried in the non-ICK segments motivated us to examine the relationship between 24 hr feeding and charge per residue (total protein charge divided by the number of amino acids) for the four proteins, as shown in Figure 2B. Interestingly, there is an approximate linear relationship, with a near four-fold increase in feeding from a doubling of the protein charge density.

Charge Modified AgRP Variants

We further tested the role of charge with a series of mutations in full $AgRP_{83-132}$. To eliminate positive charges, we replaced Arg or Lys with Gln, which retains local side chain steric features and preserves solubility in

aqueous solution (Table 1). AgRP-2Q lacks two charges in the C-terminal loop, whereas AgRP-4Q lacks charges in both the N-terminal segment and the C-terminal loop. Feeding behavior after ICV injection is shown in Figure 3A. Both AgRP and AgRP-2Q greatly stimulate feeding in the first 24 hours. Consistent with the data of Figure 2, basic residues within the C-terminal loop are not important for the initial feeding response. Interestingly, AgRP-2Q is somewhat more potent than wild type in both short and long term feeding responses. In contrast, AgRP-4Q gives a weak 24 hour response ($P<0.05$) and returns to baseline after the second day. AgRP-4Q elicits responses similar to that of $AgRP_{87-120}$ demonstrating that elimination of the non-ICK segments, or simply the basic residues within these segments, is sufficient to reduce both short and long term potency.

To further test the relationship between positive charge and feeding stimulation, we developed AgRP analogues with additional Lys residues. Inspection of the wild type $AgRP_{83-132}$ three dimensional structure reveals a cluster of basic residues extending from the active loop (Figure 1) to the end of the C-terminal loop, as shown in Figure 4. We reasoned that this conserved spatial arrangement could play a part in the feeding enhancement observed for $AgRP_{83-132}$ relative to $AgRP_{83-120}$. Consequently, we considered positions contiguous with this cluster. Among the possible positions, we chose to mutate Gly123 and Ala125 since these amino acids lack side chain functional groups and are therefore unlikely to play a structural role. The

resulting double mutant is referred to as AgRP-2K. We additionally replaced the two Ser residues in the N-terminal segment with Lys, giving the AgRP-4K analog.

The results following ICV injection of AgRP-2K and AgRP-4K are striking, as shown in Figure 3B. AgRP-2K elicits an approximate 50% increase in food uptake relative to wild type AgRP in the first 24 hours ($P<0.001$), and continues to stimulate feeding out to six or seven days. The initial response from AgRP-4K is similar to that of AgRP-2K, but here the animals display elevated feeding beyond nine days, at which point the experiments were halted ($P<0.05$ at day 8). The relationship between 24 hour feeding and charge density in the Gln and Lys mutants is displayed in Figure 3C and supports linear behavior observed for the truncated AgRP variants. Finally, we examined the change in body mass five days after injection, as shown in Figure 4D. The results parallel the relationship observed between charge and 24 hour feeding (Figure 3E), with AgRP-4Q giving a slight decrease in body mass, and AgRP-4K giving by far the greatest increase. Moreover, AgRP-4K leads to an increase in body mass that is approximately double that observed for wild type $AgRP_{83-132}$. ICV data are fully summarized in Table 2.

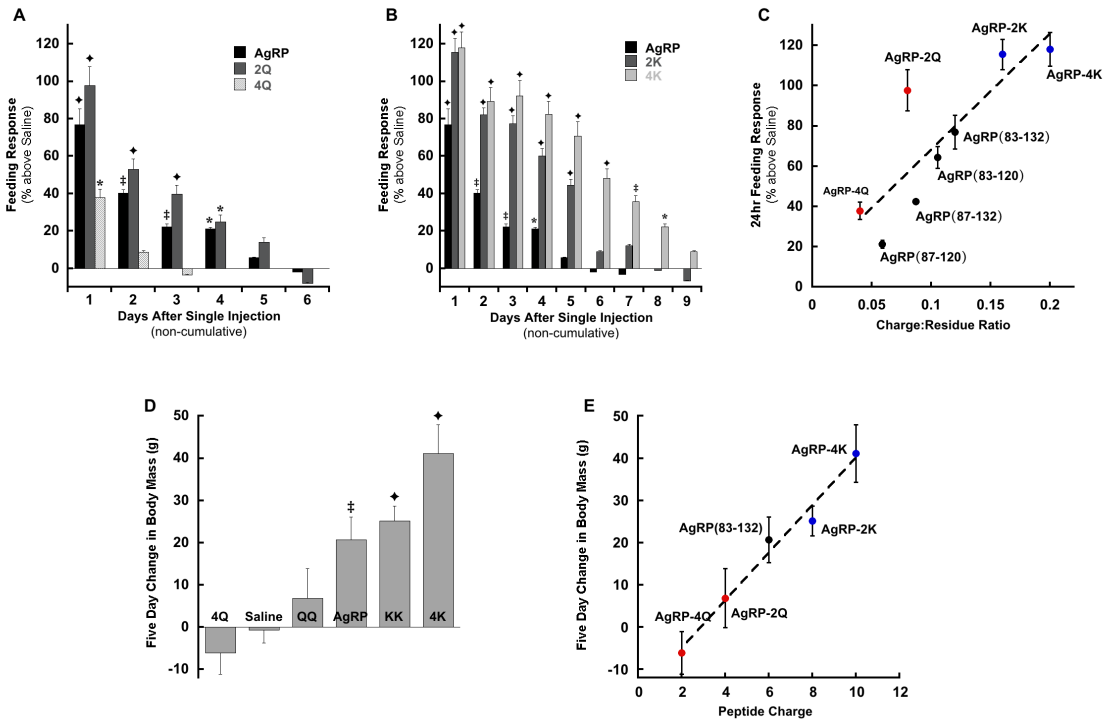

Figure 3. Effect of a single administration of a 1.0 mmol dose of mutated and designed AgRPs into third cerebral ventricle in male Long-Evans rats. (A and B) Non-cumulative percent increase of feeding response compared to saline of AgRP proteins with modified charges. (C) Relationship between 24 hr feeding and net charge density for all AgRP constructs. (D) 5-Day change in body mass and (E) trend in net peptide charge and 5-day change in body mass. ✦ $P < 0.001$, ‡ $P < 0.01$, and * $P < 0.05$ vs saline.

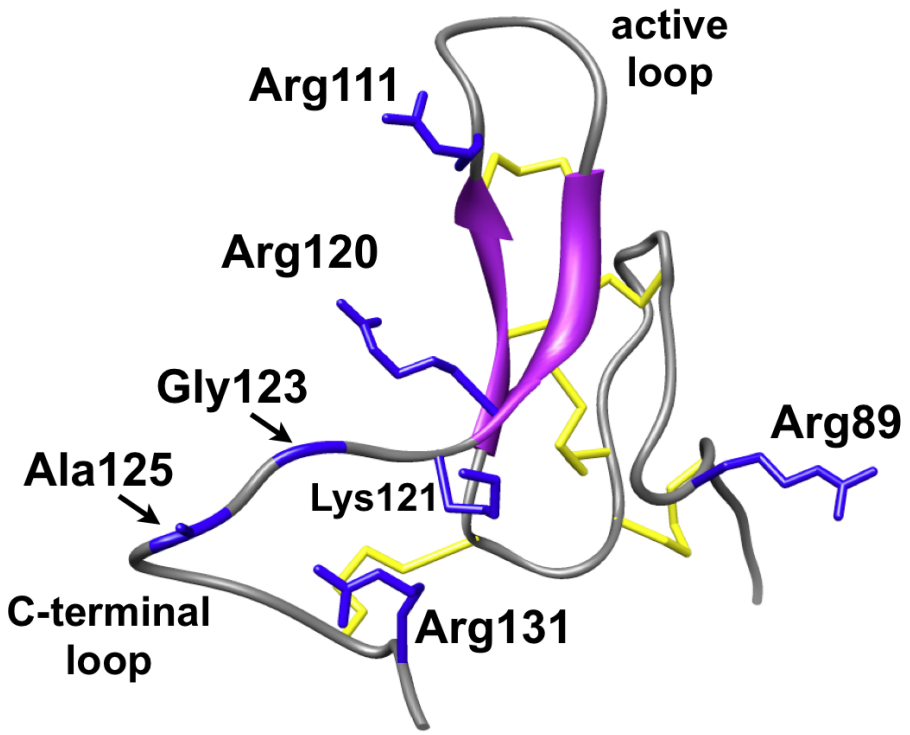

Figure 4. Cluster of basic residues (blue) in AgRP(83-132) from the active and C-terminal loops. AgRP-2K was developed by mutation of Gly123 and Ala125 (arrows) to Arg. Basic residue side chains in the N-terminal segment (Ser^{83}-Ser^{84}-Arg^{85}-Arg^{86}) are not shown.

Table 2 ICV Feeding and Body Mass

Peptide	24hr Feeding (% above Saline)	Day-3 Feeding (% above Saline)	Day-5 Feeding (% above Saline)	5–Day ΔBody Mass (g)
AgRP(83-132)	76.94 ± 8.4✦	22.24 ± 0.9‡	5.78 ± 0.3*	20.7 ± 5.4‡
AgRP(87-132)	42.4 ± 1.1✦	5.02 ± 0.4*	–	ND
AgRP(83-120)	64.33 ± 5.4✦	13.49 ± 1.5*	–	ND
AgRP(87-120)	21.32 ± 2#	11.60 ± 0.5#	–	ND
AgRP-2Q	97.7 ± 10.1✦	39.84 ± 4.6✦	14.07 ± 2.3#	6.89 ± 7#
AgRP-4Q	37.9 ± 4.4*	-3.45 ± 0.2#	–	-6.09 ± 5#
AgRP-2K	115.5 ± 7.5✦	77.28 ± 4.3✦	44.51 ± 3.1✦	25.16 ± 3.5✦
AgRP-4K	118 ± 8.3✦	92.27 ± 8.3✦	70.78 ± 7.6✦	41.11 ± 6.8✦

ND, Not Determined

✦ $P < 0.001$, ‡ $P < 0.01$, * $P < 0.05$, and # $P \geq 0.2$ vs saline

Mc3R and Mc4R Pharmacology

We used both displacement and activity assays to evaluate the influence of truncation or charge alteration on receptor pharmacology. Measurements were performed on HEK293 cells expressing the desired receptor subtype. Figure 5 shows ^{125}I-NDP-MSH displacement for all variants at Mc3R and Mc4R, with K_i values and errors reported in Table 2. Variation is limited from 4.5 to 16 nM at Mc3R, and from 7.6 to 16 nM at Mc4R. The variants that give the strongest feeding response fall in the middle of the K_i range and, in general, do not suggest any relationship between dissociation constant and short term or long term consumption. Each variant was further evaluated for its ability to suppress NDP-MSH stimulated cAMP production. Antagonists give a rightward shift in the response curve. The resulting curves are shown in Figure 5, with EC_{50} values and errors in Table 3. The EC_{50} values also exhibit limited variation, although greater than observed for the displacement studies, and range from 1.6 to 16 nM at Mc3R, and 1.7 to 17 nM at Mc4R. Interestingly, the lowest EC_{50} values at both receptors are observed for the AgRP-4Q and AgRP-4K variants, which elicit opposite feeding responses. In general, these results are consistent with our previous work, which found equivalent receptor affinity between $AgRP_{87\text{-}120}$ and $AgRP_{87\text{-}132}$, and demonstrate that receptor affinity or activity cannot account for the broad range of *in vivo* responses observed for the panel of AgRP variants.

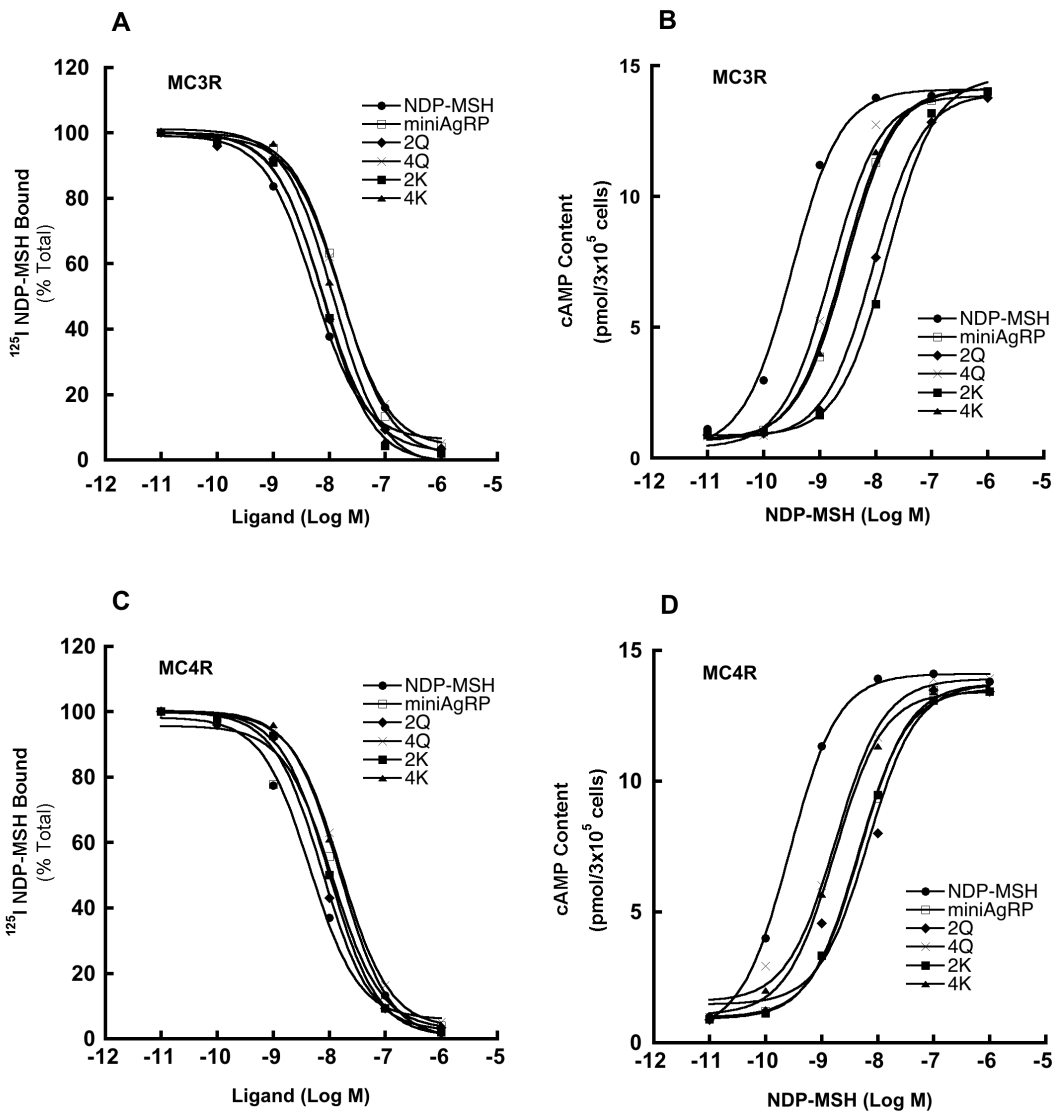

Figure 5. Pharmacology of novel AgRP constructs at Mc3R and Mc4R. (A & C) Displacement of ^{125}I-NDP-MSH; (C & D) cAMP production from increasing NDP-MSH concentrations in the presence of 0.10 μM AgRP proteins.

Table 3 Ligand Displacement and EC50 Values

	Mc3R		Mc4R	
Peptide	K_i (nM)	EC_{50} (nM)	K_i (nM)	EC_{50} (nM)
AgRP(83-132)	ND	ND	11 ± 0.7[d]	ND
AgRP(87-132)	5.2 ± 0.7[a]	8.9 ± 0.2[c]	11 ± 1[a]	17 ± 3[b]
AgRP(83-120)	16.5 ± 0.4	2.96 ± 0.4	11.4 ± 4	4.92 ± 1.3
AgRP(87-120)	7.5 ± 0.5[a]	5.5 ± 0.2	6.1 ± 0.5[a]	13 ± 3[b]
AgRP-2Q	7.56 ± 1.3	9.22 ± 1.4	7.56 ± 0.3	6.66 ± 2.1
AgRP-4Q	15.6 ± 0.3	1.62 ± 0.3	16.2 ± 0.7	1.8 ± 0.5
AgRP-2K	7.84 ± 0.5	16.1 ± 1.6	9.99 ± 3.7	4.54 ± 1.3
AgRP-4K	11.91 ± 4	2.66 ± 0.3	15.65 ± 1.4	1.72 ± 0.4

ND, Not Determined

[a] Data adapted from Jackson et al. (*17*)

[b] Data adapted from Patel et al. (*16*)

[c] Data adapted from Wilczynski et al. (*34*)

[d] Data adapted from Creemers et al. (*11*)

Possible Mechanisms and Implications

The findings above identify an unanticipated but nevertheless dramatic functional role for the AgRP polypeptide segments outside of the ICK core domain. Comparison of wild type AgRP to a mini-AgRP, composed of only the ICK core, shows that the Ser-Ser-Arg-Arg N-terminal extension and the C-terminal loop greatly enhance both the initial and long-term feeding responses. Of these two non-ICK segments, the N-terminal extension is more important, especially for the initial feeding response, but both play a role in sustaining feeding levels above baseline. By evaluation of designed AgRP mutants, we further showed that positive charge conferred by basic residues in these segments is responsible for the observed *in vivo* responses. Inclusion of additional charges beyond those found in wild type results in a protein that generates a profound feeding response that lasts almost twice as long as that induced by the wild type AgRP. It is unlikely that these results arise from modulation in receptor binding affinity, as the measured dissociation constants and cAMP activities at Mc3R and Mc4R exhibit little variation and no correlation with feeding behavior.

Examination of mammalian AgRP sequences reveals some variation in the two non-ICK segments, but always at positions that do not carry positive charge (Table 1) (*12, 13*). The basic Lys and Arg residues are completely conserved, and acidic residues are never found at sites that do exhibit variation. It is unlikely that these segments play a structural role.

Structure determination by NMR, performed by our lab, found that the C-terminal loop is flexible and points away from the ICK core containing four of the five disulfide bonds (*13*). Moreover, the mini-AgRP construct folds cooperatively with stability that is indistinguishable from $AgRP_{83-132}$ (*17*). Interestingly, the mini-AgRP core domain is so stable that it is now being used as a scaffold in protein design (*20*-*22*).

There is also no evidence that these segments are required for in vivo processing to produce mature $AgRP_{83-132}$. As noted in the Introduction, AgRP is produced as a pro-protein that undergoes processing by the serine endoprotease PC 1/3 (*11, 12*). AgRP residues 79 – 82 (Arg-Glu-Pro-Arg) follow the P4-P1 consensus sequence targeting cleavage to the Arg82-Ser83 peptide bond (*23, 24*). Alternate cleavage sights are not observed; the processed form of the protein is found exclusively as $AgRP_{83-132}$ (*25*). Moreover, PC 1/3 is tolerant of sequence variations at the P1'-P4' sites (Ser-Ser-Arg-Arg in AgRP) following the cleavage point, thus suggesting a distinct role for the conserved Arg85-Arg86 residues (*23*).

Among the known collection of natural and synthetic orexigenic peptides, AgRP exhibits the greatest overall potency. For example, a single 1.0 nM dose of neuropeptide Y (NPY) rapidly stimulates feeding beyond that of an equivalent dose of AgRP, but its effects quickly dissipate and feeding returns to baseline after 24 hours (*10, 26*). The synthetic cyclic hexapeptide SHU9119 gives a long-term response similar to AgRP, but requires higher

minimal doses for activation (*8*). Because of its unique behavior, AgRP is considered to be an important lead in the development of drugs for treating cachexia (*27*). Cachexia is a state of negative energy balance that often arises with cancer, AIDS, kidney failure and leads to malnutrition and loss of body mass (*7, 28*). Maintaining positive energy balance, on the other hand, correlates strongly with the outcome of cancer patients undergoing radiation or chemotherapy. Consistent with the role of the melanocortin system in maintaining energy balance, animal models driven to cachexia by tumors or administration of lipopolysaccharide (LPS) resume normal feeding and body weight from the administration of Mc4R antagonists, including AgRP (*27*). It is therefore noteworthy that our findings here identify new features that enhance AgRP function and prolong efficacy by nearly a factor of two.

It is clear from our experiments that AgRP's basic residues, outside of the ICK core McR recognition domain, play a central role in modulating short- and long-term AgRP function. Although the direct mechanism linking positive charge to AgRP function is not clear, we note three possibilities. First, the basic residues may increase AgRP diffusibility thereby moving the protein more efficiently from the ventricle to the hypothalamus. Second, they may slow degradation or facilitate interactions with accessory molecules proximal to the melanocortin receptors. For example, negatively charged syndecans, cell surface proteoglycans, are implicated in McR regulation (*29, 30*). New experiments show that AgRP localization in the paraventricular nucleus is

reduced in syndecan knockout mice, suggesting that syndecans are required for concentrating AgRP at postsynaptic membranes (*31*). Finally, the basic residues may facilitate signaling through a non-McR pathway. In support of this mechanism, injection of the synthetic agonist MTII, following AgRP administration, transiently reduces feeding, which then returns to the level consistent with AgRP dose (*10*). Moreover, loss of feeding regulation, resulting from selective ablation of AgRP neurons, is not reversed by increased ASIP levels (*32*).

In summary, we have demonstrated a clear functional role for AgRP's conserved non-ICK segments. The basic, positively charged residues are vital for AgRP stimulated long-term feeding. Enhancement of positive charge in these non-ICK segments leads to a protein of unprecedented orexigenic potency. Moreover, AgRP may be engineered to have variable long-term feeding profiles. Given that the arcuate nucleus is not fully protected by the blood brain barrier, the potent AgRP-4K protein developed here, or its derivatives, may be deliverable by intravenous injection. In general, the principles identified here will be helpful in pharmaceutical design for treating cachexia and perhaps other conditions associated with improper energy balance.

Acknowledgements

The authors thank Professor Greg Barsh of Stanford University and the HudsonAlpha Institute for helpful discussion and comments on the manuscript. This work was supported by a grant from the National Institutes of Health (DK064265).

References

1. Kaelin, C. B., Candille, S. I., Yu, B., Jackson, P., Thompson, D. A., Nix, M. A., Binkley, J., Millhauser, G. L., and Barsh, G. S. (2008) New ligands for melanocortin receptors, *Int J Obes (Lond) 32 Suppl 7*, S19-27.

2. Ollmann, M. M., Wilson, B. D., Yang, Y. K., Kerns, J. A., Chen, Y., Gantz, I., and Barsh, G. S. (1997) Antagonism of central melanocortin receptors in vitro and in vivo by agouti-related protein, *Science (New York, NY) 278*, 135-138.

3. Wilson, B. D., Ollmann, M. M., and Barsh, G. S. (1999) The role of agouti-related protein in regulating body weight, *Mol Med Today 5*, 250-256.

4. Katsuki, A., Sumida, Y., Gabazza, E. C., Murashima, S., Tanaka, T., Furuta, M., Araki-Sasaki, R., Hori, Y., Nakatani, K., Yano, Y., and Adachi, Y. (2001) Plasma levels of agouti-related protein are increased in obese men, *J Clin Endocrinol Metab 86*, 1921-1924.

5. Adan, R. A., Hillebrand, J. J., De, R. C., Nijenhuis, W., Vink, T., Garner, K. M., and Kas, M. J. (2003) Melanocortin system and eating disorders, *Annals of the New York Academy of Sciences 994*, 267-274.

6. Vink, T., Hinney, A., van, E. A. A., van, G. S. H., Sandkuijl, L. A., Sinke, R. J., Herpertz-Dahlmann, B. M., Hebebrand, J., Remschmidt, H., van, E. H., and Adan, R. A. (2001) Association between an agouti-related protein gene polymorphism and anorexia nervosa, *Mol Psychiatry 6*, 325-328.

7. Krasnow, S. M., and Marks, D. L. (2010) Neuropeptides in the pathophysiology and treatment of cachexia, *Current Opinion in Supportive and Palliative Care 4*, 266-271.

8. Joppa, M. A., Ling, N., Chen, C., Gogas, K. R., Foster, A. C., and Markison, S. (2005) Central administration of peptide and small molecule MC4 receptor antagonists induce hyperphagia in mice and attenuate cytokine-induced anorexia, *Peptides 26*, 2294-2301.

9. Hagan, M. M., Benoit, S. C., Rushing, P. A., Pritchard, L. M., Woods, S. C., and Seeley, R. J. (2001) Immediate and prolonged patterns of Agouti-related peptide-(83--132)-induced c-Fos activation in hypothalamic and extrahypothalamic sites., *Endocrinology 142*, 1050-1056.

10. Hagan, M. M., Rushing, P. A., Pritchard, L. M., Schwartz, M. W., Strack, A. M., van der Ploeg, L. H., Woods, S. C., and Seeley, R. J. (2000) Long-term orexigenic effects of AgRP-(83---132) involve mechanisms other

than melanocortin receptor blockade., *American journal of physiology Regulatory, integrative and comparative physiology 279*, R47-52.

11. Creemers, J. W., Pritchard, L. E., Gyte, A., Le, R. P., Meulemans, S., Wardlaw, S. L., Zhu, X., Steiner, D. F., Davies, N., Armstrong, D., Lawrence, C. B., Luckman, S. M., Schmitz, C. A., Davies, R. A., Brennand, J. C., and White, A. (2006) Agouti-related protein is posttranslationally cleaved by proprotein convertase 1 to generate agouti-related protein (AGRP)83-132: interaction between AGRP83-132 and melanocortin receptors cannot be influenced by syndecan-3, *Endocrinology 147*, 1621-1631.

12. Jackson, P. J., Douglas, N. R., Chai, B., Binkley, J., Sidow, A., Barsh, G. S., and Millhauser, G. L. (2006) Structural and molecular evolutionary analysis of Agouti and Agouti-related proteins, *Chemistry & biology 13*, 1297-1305.

13. McNulty, J. C., Thompson, D. A., Bolin, K. A., Wilken, J., Barsh, G. S., and Millhauser, G. L. (2001) High-resolution NMR structure of the chemically-synthesized melanocortin receptor binding domain AGRP(87-132) of the agouti-related protein, *Biochemistry 40*, 15520-15527.

14. McNulty, J. C., Jackson, P. J., Thompson, D. A., Chai, B., Gantz, I., Barsh, G. S., Dawson, P. E., and Millhauser, G. L. (2005) Structures of the agouti signaling protein, *Journal of molecular biology 346*, 1059-1070.

15. He, L., Gunn, T. M., Bouley, D. M., Lu, X. Y., Watson, S. J., Schlossman, S. F., Duke-Cohan, J. S., and Barsh, G. S. (2001) A biochemical function for attractin in agouti-induced pigmentation and obesity, *Nature genetics 27*, 40-47.

16. Patel, M. P., Cribb Fabersunne, C. S., Yang, Y.-K., Kaelin, C. B., Barsh, G. S., and Millhauser, G. L. (2010) Loop-swapped chimeras of the agouti-related protein and the agouti signaling protein identify contacts required for melanocortin 1 receptor selectivity and antagonism, *Journal of molecular biology 404*, 45-55.

17. Jackson, P. J., McNulty, J. C., Yang, Y.-K., Thompson, D. A., Chai, B., Gantz, I., Barsh, G. S., and Millhauser, G. L. (2002) Design, pharmacology, and NMR structure of a minimized cystine knot with agouti-related protein activity, *Biochemistry 41*, 7565-7572.

18. Tota, M. R., Smith, T. S., Mao, C., MacNeil, T., Mosley, R. T., van der Ploeg, L. H., and Fong, T. M. (1999) Molecular interaction of Agouti

protein and Agouti-related protein with human melanocortin receptors, *Biochemistry 38*, 897-904.

19. Chai, B.-X., Neubig, R. R., Millhauser, G. L., Thompson, D. A., Jackson, P. J., Barsh, G. S., Dickinson, C. J., Li, J.-Y., Lai, Y.-M., and Gantz, I. (2003) Inverse agonist activity of agouti and agouti-related protein., *Peptides 24*, 603-609.

20. Jiang, L., Kimura, R. H., Miao, Z., Silverman, A. P., Ren, G., Liu, H., Li, P., Gambhir, S. S., Cochran, J. R., and Cheng, Z. (2010) Evaluation of a (64)Cu-labeled cystine-knot peptide based on agouti-related protein for PET of tumors expressing alphavbeta3 integrin, *J Nucl Med 51*, 251-258.

21. Silverman, A. P., Kariolis, M. S., and Cochran, J. R. (2011) Cystine-knot peptides engineered with specificities for alpha(IIb)beta(3) or alpha(IIb)beta(3) and alpha(v)beta(3) integrins are potent inhibitors of platelet aggregation, *J Mol Recognit 24*, 127-135.

22. Silverman, A. P., Levin, A. M., Lahti, J. L., and Cochran, J. R. (2009) Engineered cystine-knot peptides that bind alpha(v)beta(3) integrin with antibody-like affinities, *Journal of molecular biology 385*, 1064-1075.

23. Duckert, P., Brunak, S., and Blom, N. (2004) Prediction of proprotein convertase cleavage sites, *Protein Eng Des Sel 17*, 107-112.

24. Taylor, N. A., Van, D. V. W. J., and Creemers, J. W. (2003) Curbing activation: proprotein convertases in homeostasis and pathology, *Faseb J 17*, 1215-1227.

25. Breen, T. L., Conwell, I. M., and Wardlaw, S. L. (2005) Effects of fasting, leptin, and insulin on AGRP and POMC peptide release in the hypothalamus, *Brain research 1032*, 141-148.

26. Flynn, M. C., Plata-Salaman, C. R., and Ffrench-Mullen, J. M. (1999) Neuropeptide Y-related compounds and feeding, *Physiol Behav 65*, 901-905.

27. Marks, D. L., Ling, N., and Cone, R. D. (2001) Role of the central melanocortin system in cachexia, *Cancer research 61*, 1432-1438.

28. Grossberg, A. J., Scarlett, J. M., and Marks, D. L. (2010) Hypothalamic mechanisms in cachexia, *Physiol Behav 100*, 478-489.

29. Reizes, O., Benoit, S. C., Strader, A. D., Clegg, D. J., Akunuru, S., and Seeley, R. J. (2003) Syndecan-3 modulates food intake by interacting

with the melanocortin/AgRP pathway, *Annals of the New York Academy of Sciences 994*, 66-73.

30. Reizes, O., Lincecum, J., Wang, Z., Goldberger, O., Huang, L., Kaksonen, M., Ahima, R., Hinkes, M. T., Barsh, G. S., Rauvala, H., and Bernfield, M. (2001) Transgenic expression of syndecan-1 uncovers a physiological control of feeding behavior by syndecan-3, *Cell 106*, 105-116.

31. Zheng, Q., Zhu, J., Shanabrough, M., Borok, E., Benoit, S. C., Horvath, T. L., Clegg, D. J., and Reizes, O. (2010) Enhanced anorexigenic signaling in lean obesity resistant syndecan-3 null mice, *Neuroscience 171*, 1032-1040.

32. Wu, Q., Howell, M. P., Cowley, M. A., and Palmiter, R. D. (2008) Starvation after AgRP neuron ablation is independent of melanocortin signaling, *Proc Natl Acad Sci U S A 105*, 2687-2692.

33. Yang, Y. K., Ollmann, M. M., Wilson, B. D., Dickinson, C., Yamada, T., Barsh, G. S., and Gantz, I. (1997) Effects of recombinant agouti-signaling protein on melanocortin action., *Molecular endocrinology (Baltimore, Md.) 11*, 274-280.

34. Wilczynski, A., Wang, X. S., Joseph, C. G., Xiang, Z., Bauzo, R. M., Scott, J. W., Sorensen, N. B., Shaw, A. M., Millard, W. J., Richards, N. G., and Haskell-Luevano, C. (2004) Identification of putative agouti-related protein(87-132)-melanocortin-4 receptor interactions by homology molecular modeling and validation using chimeric peptide ligands, *Journal of medicinal chemistry 47*, 2194-2207.

CHAPTER 6

Summary and Conclusions

Zebrafish AgRP2

Mammalian species contain two melanocortin antagonist sequences, Agouti-signaling protein (ASIP) and Agouti-related protein (AgRP), however recent genetic analysis of teleost fish has revealed the presence of a third agouti-like protein sequence, AgRP2. Here we found that the C-terminal domain, as defined by the cysteine spacing, of the zebrafish AgRP2 exhibits similar oxidative folding properties to that of human AgRP. This new agouti sequence is able to antagonize α-MSH stimulation of cAMP at the zebrafish melanocortin 1 receptor (Mc1R), but displays no activity at any of the other melanocortin receptors. This protein is highly expressed in the pineal gland of zebrafish embryos when grown in a white background, and helps to regulate the expression of other pigment concentrating genes. These results elucidate a novel mechanism for the background pigment adaptation mechanism of lower vertebrates by which the melanocortin system is activated by direct photic inputs.

β-MSH and Obesity

The proopiomelanocortin (POMC) is a secreted hormone that is enzymatically processed by prohormone convertases to release various melanocortin agonist peptides. Here we identify significance for β-MSH in the signaling pathway at Mc4R in the hypothalamus. Genetic analysis of a small population of UK children with early-onset obesity revealed several carriers of

a POMC mutation affecting the coding region of β-MSH, causing Tyr221 to be changed to a cysteine. NMR studies reveal a loss of turn propensity following the mutation as compared to wild-type, suggesting that the tyrosine residue is required for local structure and full agonist activity.

AgRP and Glycosaminoglycans

Here we detail the expression protocol of a full-length AgRP sequence with TEV-protease recognition site designed to release the native C-terminal domain (AgRP 83-132) and the unstructured N-terminal domain. This TEV-protease is cheaper and more efficient than previously described proteases which act on the wild-type protein. Furthermore, Isothermal Titration Calorimetry (ITC) experiments on the resulting proteins and a minimized C-terminal peptide suggest a functional role for the C-loop of AgRP in binding to glycosaminoglycans.

Super AgRP Feeding Stimulation

The Agouti-related protein (AgRP) has long been implicated in the regulation of energy balance and homeostasis. The orexigenic properties of AgRP have made it a target in the development of therapies for negative metabolic disorders. Here we characterize the physiological significance of the non-ICK regions of AgRP in the stimulation of appetite. Rat feeding studies demonstrate that truncation of the short N-terminal extension (83-86)

or the C-loop (121-132) dramatically diminished the AgRP induced feeding response. We propose that the conserved basic residues (Arg and Lys) in these two regions mediate this feeding response and further characterize multiple charge variant AgRP constructs. Both of the charge-positive peptides (AgRP-2K and AgRP-4K) exhibit dramatically increased short-term (1 day) and long-term (5+ days) feeding responses. This work may provide valuable insights to the design of pharmaceutical therapies for metabolic disorders like cachexia and severe anorexia.